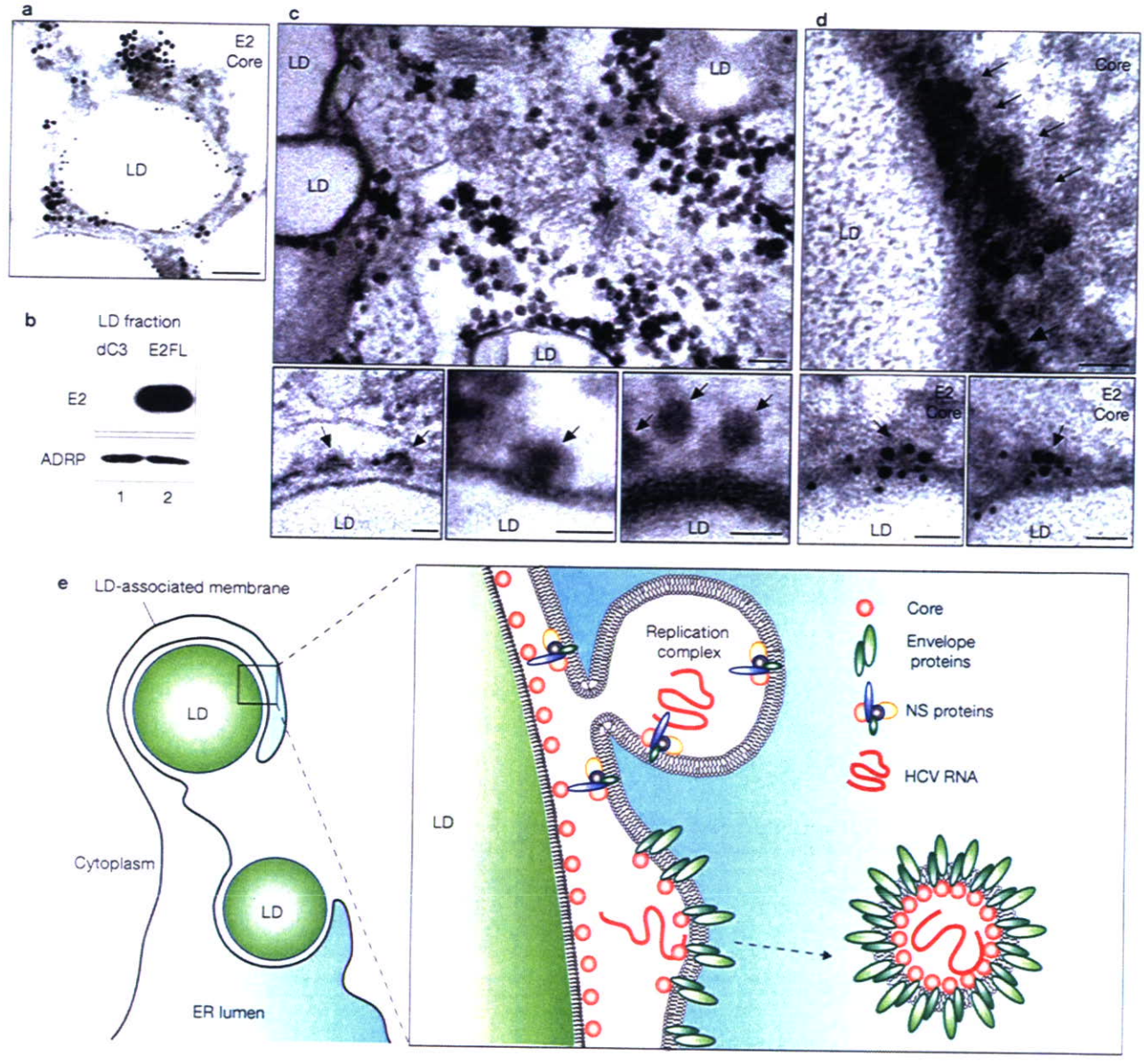

Figure 5 Virus-assembly takes place around the LDs. (**a**) Immunoelectron microscopic detection of E2 and Core in JFH1^{E2FL}-replicating cells. E2 and Core are labelled with 15 nm and 10 nm gold particles, respectively. (**b**) Western blot analysis of the lipid droplet (LD) fraction from JFH1^{E2FL} and JFH1^{dC3} replicon-bearing cells with anti-E2 and anti-ADRP antibodies. (**c**) Transmission electron micrographs of JFH1^{E2FL}-replicating cells. Arrows indicate virus-like particles. (**d**) Immunoelectron micrographs of LDs labelled with antibodies against Core (10 nm) and E2 (15 nm) are shown. Arrows show Core in electron-dense granules. Scale bar: **a** and upper panel of **c**: 100 nm; in **d** and lower panels of **c**: 50 nm. (**e**) A model for the production of infectious hepatitis C virus (HCV). Core mainly localizes on the monolayer membrane that surrounds the LD. HCV induces the apposition of the LD to the endoplasmic reticulum (ER)-derived bilayer membranes (LD-associated membrane). Core recruits NS proteins, as well as replication complexes, to the LD-associated membrane. NS proteins around the LD can then participate in infectious virus production. E2 also localizes around the LD. Through these associations, virion assembly proceeds in this local environment. Uncropped images of gels are shown in Supplementary Information Fig. S6.

larger than that of Core (Fig. 3b). The LD-proximal NS5A signal partially overlapped with the Core signal (Fig. 3b, c, grey). This concentric staining pattern was also observed with the other NS proteins (Supplementary Information, Fig. S5a), indicating that NS proteins associate with Core on the surface of LDs. Electron microscopic analysis only rarely revealed a close association of LDs with other organelles in naïve Huh-7 cells (Fig. 3d, f). However, in the case of JFH1^{E2FL}-replicating cells, about 30% of the LDs were in close proximity to membrane cisternae (Fig. 3e, arrows; 3f), arguing for a HCV-induced membrane rearrangement around LDs. Core was mainly located on the periphery of LDs, and occasionally signals were observed in more distal areas of the LDs (Fig. 3g, arrowheads and arrows, respectively). Although some NS5A signals were observed on the surface of the LD, the majority of NS5A signals were detected more distal of LDs (Fig. 3h, i). Furthermore, we often observed membrane cisternae as white lines in the same area as NS5A signals (Fig. 3i, arrows). When the same section was labelled with anti-Core and anti-NS5A antibodies, Core was detected on the surface of the LDs, whereas NS5A was mainly observed in the peripheral area of the LDs (Fig. 3j, arrowheads and arrows, respectively). In summary, these results show that Core recruits NS proteins, as well as HCV replication complexes, to the LD-associated membranes.

The above results prompted us to ask whether Core–LD colocalization is important for the production of infectious virus particles. JFH1^{E2FL}-replicating cells released virions into the culture medium and these viruses were highly infectious for naïve Huh-7.5 cells[11,21], although culture medium from JFH1$^{PP/AA}$- or JFH1$^{\Delta C3}$-replicating cells did not contain significant levels of HCV RNA and infectious virus (Fig. 4a). However, following trans-complementation with Core^{Wt}, a high titre of HCV RNA and infectious virus could be rescued from JFH1$^{\Delta C3}$-replicating cells (Fig. 4b; and see Supplementary Information, Fig. S5b, c). In contrast, the production of infectious viruses was not rescued by trans-complementation with Core$^{PP/AA}$ (Fig. 4b). RNA-binding properties and oligomerization of Core^{Wt} and Core$^{PP/AA}$, which are both necessary for virus assembly, were similar (Supplementary Information, Fig. S5d; ref. 22), arguing that the primary defect of this mutant in preventing infectious virus production is the inability to associate with LDs.

To investigate the contribution of NS proteins around LDs to infectious virus production, we used variants of NS5A, which were not recruited to LDs even in the presence of Core. We assumed that NS5A was crucial for recruiting other NS proteins to LDs, because the level of NS5A recruited to LDs via Core was higher than the levels of the other recruited NS proteins (Fig. 1c, JFH1^{E2FL}). Using alanine-scanning mutagenesis within the NS5A coding region of JFH1^{E2FL}, we generated two mutants, JFH1^{AAA99} and JFH1^{AAA102}, in which the amino-acid sequence APK (aa 99–101 of NS5A) or PPT (aa 102–104 of NS5A) was replaced by AAA (Supplementary Information, Fig. S1). In JFH1^{AAA99}- and JFH1^{AAA102}-replicating cells, NS5A was rarely detected around LDs, whereas Core was still localized to LDs (Fig. 4c, d). Importantly, these mutations impaired not only the NS5A association with LDs, but also the recruitment of other NS proteins and viral RNAs to LDs (Fig. 4d). These results indicate that NS5A is a key protein that recruits replication complexes to LDs. Importantly, HCV RNA synthesis activity in the LD fractions from these mutant JFH1-replicating cells was also severely impaired (Fig. 4e), corroborating the lack of association of HCV replication complexes with LDs.

To investigate the infectious virus production of these NS5A mutants, we prepared cells expressing similar levels of HCV proteins and RNA by adjusting the amount of transfected HCV RNA (Fig. 4e). This was necessary, because replication activities of these mutants were lower compared with JFH1^{E2FL}. Under these conditions, the amounts of Core and HCV RNA that were released into the culture medium from cells transfected with the mutants were comparable to JFH^{E2FL} (Fig. 4f, upper graph). However, infectivity titres of the mutants were severely reduced (Fig. 4f, lower panels). In sucrose density-gradient centrifugation of culture medium from JFH1^{E2FL}-bearing cells, two types of HCV particles were detected: low-density particles (about 1.12 g ml^{-1}) with high infectivity (Fig. 4g, green area of JFH1^{E2FL}), and high-density particles (about 1.15 g ml^{-1}) without infectivity (yellow area). This result indicates that only a minor portion of released HCV particles is infectious, whereas the majority of released particles lack infectivity. In contrast, cells bearing the JFH1^{AAA99} mutant almost exclusively released non-infectious particles of around 1.15 g ml^{-1}, whereas infectious particles were barely detectable (Fig. 4g, JFH1^{AAA99}). Taken together, these results provide convincing evidence that the association of NS proteins and replication complexes around LDs is critical for producing infectious viruses, whereas production of non-infectious viruses seems to follow a different pathway.

The results described so far imply that some step(s) of HCV assembly take place around LDs. To explore this possibility, we analysed the distribution of the major envelope protein E2 around the LD. Electron microscopic analysis revealed that, in about 90% of JFH1^{E2FL}-replicating cells, E2 was localized in the peripheral area of the LDs (Fig. 5a, large grains). This labelling pattern was similar to the one observed for NS5A (Fig. 3j), indicating that E2 also localizes on the LD-associated membranes. Western blot analysis of the LD fraction supported this conclusion, because the LD fraction that was purified from JFH1^{E2FL}-replicating cells, but not from JFH1$^{\Delta C3}$-replicating cells, contained E2 (Fig. 5b). Furthermore, spherical virus-like particles with an average diameter of about 50 nm were observed around LDs in JFH1^{E2FL}-replicating cells (Fig. 5c, upper panel). These particles were never observed in naïve Huh-7 cells. A more refined analysis indicates that these particles are closely associated with membranes in close proximity to LDs (Fig. 5c, lower panels, arrows). Finally, these particles around the LDs reacted with Core- and E2-specific antibodies, arguing that the particles represent true HCV virions (Fig. 5d). These results suggest that infectious HCV particles are generated from the LD-associated membranous environment.

In this study, we have demonstrated that Core recruits NS proteins, HCV RNAs and the replication complex to LD-associated membranes. Mutations of Core and NS5A (Fig. 4), which failed to associate with LDs, impaired the production of infectious virus. We note that the mutant Core retains the ability to interact with RNA (Supplementary Information, Fig. S5b) and to assemble into nucleocapside[22]. Similarly, the NS5A mutant still supports viral genome replication and the formation of capsids or virus-like particles, arguing that the introduced mutations in Core and NS5A do not affect overall protein folding, stability or function (Fig. 4). Taken together, the data show that the association of HCV proteins with LDs is important for the production of infectious viral particles (Fig. 5e).

Our results also indicate that NS proteins around the LDs participate in the assembly of infectious virus particles. In one scenario, NS proteins may indirectly contribute to the different steps of virus production — for example, by establishing the microenvironment around the LDs that is required for infectious virus production. Alternatively, NS proteins around the LDs may directly participate in virus production — for example, as components of the replication complex that provide the RNA genome to the assembling nucleocapsid.

In support of the role of LDs in virus formation, we observed that colocalization of HCV protein with LDs was low in cases of the chimera Jc1, supporting up to 1,000-fold higher infectivity titres compared with JFH1 (ref. 13). In a Jc1-infected cell, only about 20% of LDs demonstrated detectable colocalization with Core, but this value increased to 80% in the case of a Jc1 mutant lacking most of the envelope glycoprotein genes and thus being unable to produce infectious virus particles (data not shown). This inverse correlation between the efficiency of virus production and Core protein accumulation on LDs indicates that rapid assembly and virus release results in the rapid liberation of HCV proteins from the LDs.

Steatosis and abnormal lipid metabolism caused by chronic HCV infection may be linked to enhanced LD formation[14]. In fact, the overproduction of LDs is induced by Core (Supplementary Information, Fig. S3) and HCV also induces membrane rearrangements around LDs (Fig. 3d–f). Our findings suggest that excessive Core-dependent formation of LDs

and membrane rearrangements are required to supply the necessary microenvironment for virus production. NS proteins and HCV RNA seem to be translocated from the ER to the LD-associated membranes. Interestingly, the LD-associated membranes were occasionally found in continuity with ribosome-studded rough ER (Fig. 3e, arrowheads). Thus, at least parts of the LD-associated membranes are likely to be derived from ER membranes. ER marker proteins, however, were not detected in the LD fraction, suggesting that the LD-associated membrane is characteristically distinct from that of ER membranes.

To our knowledge, this is the first report showing that LDs are required for the formation of infectious virus particles. The fact that capsid protein of the hepatitis G virus also localizes to LDs[15] indicates that LDs might be important for the production of other viruses as well. Our findings demonstrate a novel function of LDs, provide an important step towards elucidating the mechanism of HCV virion production and open new avenues for novel antiviral intervention. □

METHODS

Antibodies. The antibodies used for immunoblotting and immunolabelling were specific for Core (#32-1 and RR8); E2 (AP-33 (ref. 23); 3/11, CBH5 and Flag M2 (Sigma-Aldrich, St Louis, MO); NS3 (R212)[17]; NS4A and 4B (PR12); NS5A (NS5ACL1); NS5B (NS5B-6 and JFH1-1)[24]; ADRP (Progen Biotechnik, Heidelberg, Germany); tubulin (Oncogene Research Products, MA, USA); Grp78 (StressGen, Victoria, Canada); PDI (StressGen); and Calnexin-NT (StressGen). Antibodies specific for Core (#32-1 and RR8), NS3 (R212) and NS4AB (PR12) were gifts from Dr Kohara (The Tokyo Metropolitan Institute of Medical Science, Japan). Anti-E2 antibody (AP-33) was provided by Dr Patel (MRC Virology Unit, UK). Anti-NS5B (NS5B-6) antibody was kindly provided by Dr Fukuya (Osaka University, Japan). Rabbit polyclonal antibodies specific for NS5A were raised against a bacterially expressed GST–NS5A (1–406 aa) fusion protein. In the case of the HCV chimeras Con1/C3 and H77/C3, immunofluorescence analyses were performed by using the following antibodies: Core (C7/50)[5], a JFH1 NS3-specific rabbit polyclonal antiserum; NS4B (#86)[25]; and NS5A (Austral Biologicals, San Ramon, CA).

Indirect immunofluorescence analysis. Indirect immunofluorescence analysis was performed essentially as described previously[17], with slight modifications. Cells transfected with JFH1 RNA were seeded onto a collagen-coated Labtech II 8-well chamber (Nunc, NY, USA). The coating with collagen was performed using rat-tail collagen type I (BD Bioscience, Palo Alto, CA) according to manufacturer's instructions. Three days after seeding, the cells were washed twice with phosphate-buffered saline (PBS; 137 mM NaCl, 2.7 mM KCl, 4.3 mM Na_2HPO_4 and 1.4 mM KH_2PO_4) and fixed with fixation solution (4% paraformaldehyde and 0.15 M sodium cacodylate at pH 7.4) for 15 min at room temperature. After washing with PBS, the cells were permeabilized with 0.05% Triton X-100 in PBS for 15 min at room temperature. For the precise localization of the proteins, the cells were permeabilized with 50 μg ml^{-1} of digitonin in PBS for 5 min at room temperature[26]. After incubating the cells with blocking solution (10% fetal bovine serum and 5% bovine serum albumin (BSA) in PBS) for 30 min, the cells were incubated with the primary antibodies. The fluorescent secondary antibodies were Alexa 568- or Alexa 647-conjugated anti-mouse or anti-rabbit IgG antibodies (Invitrogen, Carlsbad, CA). Nuclei were labelled with 4',6-diamidino-2-phenylindole (DAPI). LDs were visualized with BODIPY 493/503 (Invitrogen). Analyses of JFH1 were performed on a Leica SP2 confocal microscope (Leica, Heidelberg, Germany). Analysis of the Con1/C3 and the H77/C3 chimeras was performed in the same way, except that imaging was performed on a Nikon C1 confocal microscope (Nikon, Tokyo, Japan).

Electron microscopy. For conventional electron microscopy, cells cultured in plastic Petri dishes were processed *in situ*. The cells were fixed in 2.5% glutaraldehyde and 0.1 M sodium phosphate (pH 7.4), and then in OsO_4 and 0.1 M sodium phosphate (pH 7.4). The cells were then dehydrated in a graded ethanol series and embedded in an epoxy resin. Ultrathin sections were cut perpendicular to the base of the dish. For immuno-electron microscopy, cells were detached from the dish with a cell scraper after fixation in 4% paraformaldehyde, 0.1% glutaraldehyde and 0.1 M sodium phosphate (pH 7.4) for 24 h, and washed in 0.1 M lysine, 0.1 M sodium phosphate (pH 7.4) and 0.15 M sodium chloride. After dehydrating the cells in a graded series of cold ethanol, they were embedded in Lowicryl K4M at −20 °C. Ultrathin sections were labelled with primary antibodies and colloidal gold particles (15 nm) conjugated to anti-mouse IgG or anti-rabbit IgG antibodies. For double labelling, colloidal gold particles with different diameters (10 nm and 15 nm) conjugated to anti-mouse IgG or anti-rabbit antibodies were used. Samples were observed after staining with uranyl acetate and lead citrate with a JEM 1010 electron microscope at the accelerating voltage of 80 kV. Anti-Core (#32-1 and RR88), anti-NS5A (NS5ACL1) and anti-E2 (Flag M2) antibodies were used.

Preparation of the lipid droplets. Cells at a confluency of ~80% on a dish with a diameter of 14 cm were scraped in PBS. The cells were pelleted by centrifugation at 1,500 rpm. The pellet was resuspended in 500 μl of hypotonic buffer (50 mM HEPES, 1 mM EDTA and 2 mM $MgCl_2$ at pH 7.4) supplemented with protease inhibitors (Roche Diagnostics, Basel, Switzerland) and was incubated for 10 min at 4 °C. The suspension was homogenized with 30 strokes of a glass Dounce homogenizer using a tight-fitting pestle. Then, 50 μl of 10× sucrose buffer (0.2 M HEPES, 1.2 M KoAc, 40 mM $Mg(oAc)_2$ and 50 mM DTT at pH 7.4) was added to the homogenate. The nuclei were removed by centrifugation at 2,000 rpm for 10 min at 4 °C. The supernatant was collected and centrifuged at 16,000 *g* for 10 min at 4 °C. The supernatant (S16) was mixed with an equal volume of 1.04 M sucrose in isotonic buffer (50 mM HEPES, 100 mM KCl, 2 mM $MgCl_2$ and protease inhibitors). The solution was set at the bottom of 2.2-ml ultracentrifuge tube (Hitachi Koki, Tokyo, Japan). One milliliter of isotonic buffer was loaded onto the sucrose mixture. The tube was centrifuged at 100,000 *g* in an S55S rotor (Hitachi Koki) for 30 min at 4 °C. After the centrifugation, the LD fraction on the top of the gradient solution was recovered in isotonic buffer. The suspension was mixed with 1.04 M sucrose and centrifuged again at 100,000 *g*, as described above, to eliminate possible contamination with other organelles. The collected LD fraction was used for western blotting or the HCV RNA synthesis assay.

HCV RNA synthesis assay. An assay of HCV RNA synthesis using digitonin-permeabilized cells was performed as described previously[17]. For RNA synthesis assays using the LD fraction, the LD fraction collected by sucrose-gradient sedimentation was suspended in buffer B, which contained 2 mM manganese (II) chloride, 1 mg ml^{-1} acetylated BSA (Nacalai Tesque, Kyoto, Japan), 5 mM phosphocreatine (Sigma), 20 units/ml creatine phosphokinase (Sigma), 50 μg ml^{-1} actinomycin D, 500 μM ATP, 500 μM CTP, 500 μM GTP (Roche Diagnostics) and 1.85 MBq of [α-^{32}P] UTP (GE Healthcare, Little Chalfont, UK), and incubated at 27 °C for 4 h. The reaction products were analysed by gel electrophoresis followed by autoradiography.

Note: Supplementary Information is available on the Nature Cell Biology website.

ACKNOWLEDGEMENTS

We thank T. Fujimoto and Y. Ohsaki at Nagoya University for helpful discussions and technical assistance. Y.M. is a recipient of a JSPS fellowship. K.S. is supported by Grants-in-Aid for cancer research and for the second-term comprehensive 10-year strategy for cancer control from the Ministry of Health, Labour and Welfare, as well as by a Grant-in-Aid for Scientific Research on Priority Areas "Integrative Research Toward the Conquest of Cancer" from the Ministry of Education, Culture, Sports, Science and Technology of Japan. T.W. is also supported, in part, by a Grant-in-Aid for Scientific Research from the Japan Society for the Promotion of Science; and by the Research on Health Sciences Focusing on Drug Innovation from the Japan Health Sciences Foundation. R.B. is supported by the Sonderforschungsbereich 638 (Teilprojekt A5) and the Deutsche Forschungsgemeinschaft (BA1505/2-1). M.Z. and R.B. thank the Nikon Imaging Center at the University of Heidelberg for providing access to their confocal fluorescence microscopes and Ulrike Engel for the excellent support.

AUTHOR CONTRIBUTIONS

Y.M. and K.S. planned experiments and analyses. Y.M. was responsible for experiments for Figs 1, 2, 3a–c, 4a–e and 5b. K.A., N.U., electron microscopy; T.H., Fig. 1e; M.Z., R.B., Fig. S2e; and K.S. and K.W., Fig. 4f–g. T.W. provided JFH1 strain. Y.M. and K.S. wrote the manuscript. All authors discussed the results and commented on the manuscript.

COMPETING FINANCIAL INTERESTS

The authors declare no competing financial interests.

Published online at http://www.nature.com/naturecellbiology/
Reprints and permissions information is available online at http://npg.nature.com/reprintsandpermissions/

1. Martin, S. & Parton, R. G. Lipid droplets: a unified view of a dynamic organelle. *Nature Rev. Mol. Cell Biol.* **7**, 373–378 (2006).
2. Blanchette-Mackie, E. J. *et al.* Perilipin is located on the surface layer of intracellular lipid droplets in adipocytes. *J. Lipid Res.* **36**, 1211–1226 (1995).
3. Vock, R. *et al.* Design of the oxygen and substrate pathways. VI. structural basis of intracellular substrate supply to mitochondria in muscle cells. *J. Exp. Biol.* **199**, 1689–1697 (1996).
4. Liang, T. J. *et al.* Viral pathogenesis of hepatocellular carcinoma in the United States. *Hepatology* **18**, 1326–1333 (1993).
5. Moradpour, D., Englert, C., Wakita, T. & Wands, J. R. Characterization of cell lines allowing tightly regulated expression of hepatitis C virus core protein. *Virology* **222**, 51–63 (1996).
6. Deleersnyder, V. *et al.* Formation of native hepatitis C virus glycoprotein complexes. *J. Virol.* **71**, 697–704 (1997).
7. Kato, N. *et al.* Molecular cloning of the human hepatitis C virus genome from Japanese patients with non-A, non-B hepatitis. *Proc. Natl Acad. Sci. USA* **87**, 9524–9528 (1990).
8. Hijikata, M. & Shimotohno, K. [Mechanisms of hepatitis C viral polyprotein processing]. *Uirusu* **43**, 293–298 (1993).
9. Dubuisson, J., Penin, F. & Moradpour, D. Interaction of hepatitis C virus proteins with host cell membranes and lipids. *Trends Cell Biol.* **12**, 517–523 (2002).
10. Wakita, T. *et al.* Production of infectious hepatitis C virus in tissue culture from a cloned viral genome. *Nature Med.* **11**, 791–796 (2005).
11. Lindenbach, B. D. *et al.* Complete replication of hepatitis C virus in cell culture. *Science* **309**, 623–626 (2005).
12. Zhong, J. *et al.* Robust hepatitis C virus infection in vitro. *Proc. Natl Acad. Sci. USA* **102**, 9294–9299 (2005).
13. Pietschmann, T. *et al.* Construction and characterization of infectious intragenotypic and intergenotypic hepatitis C virus chimeras. *Proc. Natl Acad. Sci. USA* **103**, 7408–7413 (2006).
14. Moriya, K. *et al.* Hepatitis C virus core protein induces hepatic steatosis in transgenic mice. *J. Gen. Virol.* **78**, 1527–1531 (1997).
15. Hope, R. G., Murphy, D. J. & McLauchlan, J. The domains required to direct core proteins of hepatitis C virus and GB virus-B to lipid droplets share common features with plant oleosin proteins. *J. Biol. Chem.* **277**, 4261–4270 (2002).
16. Egger, D. *et al.* Expression of hepatitis C virus proteins induces distinct membrane alterations including a candidate viral replication complex. *J. Virol.* **76**, 5974–5984 (2002).
17. Miyanari, Y. *et al.* Hepatitis C virus non-structural proteins in the probable membranous compartment function in viral genome replication. *J. Biol. Chem.* **278**, 50301–50308 (2003).
18. Quinkert, D., Bartenschlager, R. & Lohmann, V. Quantitative analysis of the hepatitis C virus replication complex. *J. Virol.* **79**, 13594–13605 (2005).
19. Tauchi-Sato, K., Ozeki, S., Houjou, T., Taguchi, R. & Fujimoto, T. The surface of lipid droplets is a phospholipid monolayer with a unique fatty acid composition. *J. Biol. Chem.* **277**, 44507–44512 (2002).
20. Londos, C., Brasaemle, D. L., Schultz, C. J., Segrest, J. P. & Kimmel, A. R. Perilipins, ADRP, and other proteins that associate with intracellular neutral lipid droplets in animal cells. *Semin. Cell Dev. Biol.* **10**, 51–58 (1999).
21. Blight, K. J., McKeating, J. A. & Rice, C. M. Highly permissive cell lines for subgenomic and genomic hepatitis C virus RNA replication. *J. Virol.* **76**, 13001–13014 (2002).
22. Klein, K. C., Dellos, S. R. & Lingappa, J. R. Identification of residues in the hepatitis C virus core protein that are critical for capsid assembly in a cell-free system. *J. Virol.* **79**, 6814–6826 (2005).
23. Owsianka, A. *et al.* Monoclonal antibody AP33 defines a broadly neutralizing epitope on the hepatitis C virus E2 envelope glycoprotein. *J Virol* **79**, 11095–11104 (2005).
24. Ishii, N. *et al.* Diverse effects of cyclosporine on hepatitis C virus strain replication. *J. Virol.* **80**, 4510–4520 (2006).
25. Lohmann, V., Korner, F., Herian, U. & Bartenschlager, R. Biochemical properties of hepatitis C virus NS5B RNA-dependent RNA polymerase and identification of amino acid sequence motifs essential for enzymatic activity. *J Virol* **71**, 8416–8428 (1997).
26. Ohsaki, Y., Maeda, T. & Fujimoto, T. Fixation and permeabilization protocol is critical for the immunolabeling of lipid droplet proteins. *Histochem. Cell Biol.* **124**, 445–452 (2005).

THE JOURNAL OF BIOLOGICAL CHEMISTRY VOL. 282, NO. 45, pp. 32765–32772, November 9, 2007

Anti-hepatitis C Virus Activity of Tamoxifen Reveals the Functional Association of Estrogen Receptor with Viral RNA Polymerase NS5B*

Received for publication, May 30, 2007, and in revised form, August 15, 2007 Published, JBC Papers in Press, August 17, 2007, DOI 10.1074/jbc.M704418200

Koichi Watashi, Daisuke Inoue, Makoto Hijikata, Kaku Goto, Hussein H. Aly, and Kunitada Shimotohno[1]

From the Department of Viral Oncology, Institute for Virus Research, Kyoto University, 53 Kawaharacho, Shogoin, Sakyo-ku, Kyoto 606-8507, Japan

Hepatitis C virus (HCV) is a major causative agent of hepatocellular carcinoma. HCV genome replication occurs in the replication complex (RC) around the endoplasmic reticulum membrane. However, the mechanisms regulating the HCV RC remain widely unknown. Here, we used a chemical biology approach to show that estrogen receptor (ESR) is functionally associated with HCV replication. We found that tamoxifen suppressed HCV genome replication. Part of ESRα resided on the endoplasmic reticulum membranes and interacted with HCV RNA polymerase NS5B. RNA interference-mediated knockdown of endogenous ESRα reduced HCV replication. Mechanistic analysis suggested that ESRα promoted NS5B association with the RC and that tamoxifen abrogated NS5B-RC association. Thus, ESRα regulated the presence of NS5B in the RC and stimulated HCV replication. Moreover, the ability of ESRα to regulate NS5B was suggested to serve as a potential novel target for anti-HCV therapeutics.

Estrogen receptor (ESR)[2] belongs to the steroid hormone receptor family of the nuclear receptor superfamily (1). ESR consists of two subtypes, ESRα and ESRβ. As a primary physiological function, ESR is involved in the transcription for downstream genes in response to stimulation by the ligand, estradiol. In the normal state, ESR is mainly located in the cytoplasm and nucleus. Upon binding of the ligand, ESR dimerizes and translocates into the nucleus, where it binds to the ESR-responsive elements (ERE) in the DNA promoter of downstream genes and drives transcription. In addition to this classical genomic action, a portion of ESR is located on the membrane, such as the plasma membrane, and involved in the nongenomic function of triggering signal transduction pathways, such as mitogen-activated protein kinase, phosphatidylinositol 3-kinase, and protein kinase C (2–4). Although the molecular basis of ESR membrane retention is not fully understood, one mechanism involves a membrane protein, caveolin (CAV); ESRα interacted with CAV, and this interaction facilitated ESRα localization to the membrane (5, 6). It was also reported that ESRα localizes to the lipid rafts on the plasma membrane (7). The lipid rafts are microdomains of the membrane that form platforms enriched in cholesterol and glycosphingolipids. However, the characteristics and relevance of membrane-associated ESR have not been fully disclosed. Here, we report the novel role of ESRα in the regulation of viral replication.

Hepatitis C virus (HCV), a causative agent of chronic hepatitis, liver cirrhosis, and hepatocellular carcinoma, constitutes a serious health problem worldwide (8). HCV has a positive strand RNA genome that produces at least 10 functional viral proteins: core, envelope 1, envelope 2, p7, nonstructural protein 2 (NS2), NS3, NS4A, NS4B, NS5A, and NS5B (9, 10). NS5B is an RNA-dependent RNA polymerase, which plays a central role in viral genome replication (11, 12). HCV genome replication can be evaluated using a HCV subgenomic replicon system, which Lohmann *et al.* (13) first established. In this system, cells carry an HCV subgenome RNA encoding NS3 to NS5B. Using this system, it has been proposed that HCV genome replication occurs in the replication complex (RC), which contains the viral genome RNA and HCV NS proteins. The RC forms on the surface of the intracellular membranes, including the endoplasmic reticulum (ER) membrane, and is surrounded by a membrane structure (14–17). It also has been reported that HCV genome replication associates with the lipid rafts on these intracellular membranes, such as the ER membrane (14, 18). These lipid rafts accumulate CAV2, and HCV proteins involved in viral genome replication cofractionate with CAV2 (18). However, it is largely unknown how the RC is formed and under what mechanism the HCV proteins participate in the RC.

A chemical biology approach is a useful method to analyze the molecular mechanism of viral life cycles as well as cellular physiological processes (19). We employed forward chemical genetics in which we analyzed HCV replication activity as a phenotypic indicator of a cell-based assay to screen chemical

* This work was supported by grants-in-aid for cancer research and for the second term comprehensive 10-year strategies for cancer control from the Ministry of Health, Labor, and Welfare; by grants-in-aid for scientific research from the Ministry of Education, Culture, Sports, Science, and Technology; by grants-in-aid for the Research for the Future Program from the Japanese Society for the Promotion of Science; and by grants-in-aid for the Program for Promotion of Fundamental Studies in Health Science from the Organization for Pharmaceutical Safety. The costs of publication of this article were defrayed in part by the payment of page charges. This article must therefore be hereby marked "*advertisement*" in accordance with 18 U.S.C. Section 1734 solely to indicate this fact.

[1] To whom correspondence should be addressed: Dept. of Viral Oncology, Institute for Virus Research, Kyoto University, 53 Kawaharacho, Shogoin, Sakyo-ku, Kyoto 606-8507, Japan. Tel.: 81-75-751-4000; Fax: 81-75-751-3998; E-mail: kshimoto@virus.kyoto-u.ac.jp.

[2] The abbreviations used are: ESR, estrogen receptor; HCV, hepatitis C virus; RC, replication complex; ER, endoplasmic reticulum; TAM, tamoxifen; ERE, ESR-responsive element(s); CAV, caveolin; NS, nonstructural protein; MM, microsomal membrane; siRNA, small interfering RNA; si-ESR, small interfering ESR; GST, glutathione *S*-transferase; aa, amino acid(s); RT, reverse transcription; NS3, NS4A, NS4B, NS5A, and NS5B, nonstructural protein 3, 4A, 4B, 5A, and 5B, respectively.

compounds that inhibited HCV replication. Using this system, we previously identified an immunosuppressant, cyclosporin A, as an anti-HCV compound (20). We also reported that cyclophilin B regulated the RNA binding activity of NS5B (21). In the current study, this chemical screening approach linked ESRα to HCV replication. We showed that tamoxifen (TAM) suppressed HCV genome replication. Using TAM as a bioprobe, we found that ESRα interacted with NS5B and regulated the participation of NS5B in the RC.

EXPERIMENTAL PROCEDURES

Cell Culture and Transfection—Huh-7 and cured MH-14 cells (21) were cultured in Dulbecco's modified Eagle's medium (Invitrogen) supplemented with 10% fetal bovine serum, minimal essential medium nonessential amino acid (Invitrogen), and kanamycin (Meiji). MH-14 cells, carrying HCV subgenomic replicon (16), and LucNeo#2 cells, carrying luciferase-containing subgenomic replicon (22), were cultured in the same medium supplemented with 300 μg/ml G418 (Invitrogen). Hus-E7/DN24 cells, a human hepatocyte cell line established by immortalization with HPV E6E7 and hTERT from human primary hepatocytes and introduction with a dominant negative form of interferon regulatory factor-7 (23), were cultured with Dulbecco's modified Eagle's medium with 20 mM Hepes (Invitrogen), 15 g/ml L-proline, 0.25 g/ml insulin (Sigma), 50 nM dexamethasone (Sigma), 44 mM $NaHCO_3$, 10 mM nicotinamide, 5 ng/ml epidermal growth factor, 0.1 mM Asc-2P, 100 IU/ml penicillin G (Invitrogen), 100 μg/ml streptomycin (Invitrogen), 5% fetal bovine serum, 1% Dulbecco's modified Eagle's medium, and 2 UG/ml Fungizone (Invitrogen) (24). Plasmid transfection was performed with FuGENE 6 transfection reagent (Roche Applied Science), as described previously (25). RNA transfection was achieved using DMrie-C transfection reagent (Invitrogen), as described previously (21). siRNA was transfected by using siLentFect (Bio-Rad) (21).

Plasmid Construction—pCMV-FL-ESRα, encoding the whole open reading frame of ESRα fused with a FLAG tag, was generated by inserting the PCR product using 5′-GTTGAATTCATGACCATGACCCTCCAC-3′ and 5′-GTTGATCTCGAGTCAGACTGTGGCAGGGAAAC-3′ as primer set and human lymphocyte cDNA library (Clontech) as a template into the EcoRI-XhoI site of pCMV-FLAG vector (21). pCAG-HA-NS5B, encoding the NS5B protein fused with a hemagglutinin tag, was made by subcloning the PCR product with 5′-GTTGCGGCCGCTATGTCAATGTCCTACTCA-3′ and 5′-GTTCTCGAGTCACCGGTTGGGGAGCAGGTA-3′ as primers and pMH14 as a template into NotI-XhoI digestion of PCAG-HA vector (21). Expression plasmids for HCV NS3, NS4B, NS5A, and NS5B (pcDNA-NS3, pcDNA-NS4B, pcDNA-NS5A, and pcDNA-NS5B, respectively) were described in Ref. 21. pGEX-ESRα A/B, C, D, and E/F, expressing the fusion protein of the domain A/B, C, D, and E/F of ESRα with GST, were prepared by the insertion of the PCR product with pCMV-FL-ESRα as a template and appropriate primers into the EcoRI-XhoI site of pGEX-6P1 vector (Clontech). The expression plasmids for the point mutants of ESRα, ESRα(L540Q), ESRα(255M), and ESRα(258M), of which Leu at aa 540, IRK at aa 255–257, and DRR at aa 258–260 were replaced by Gln, TGT, and ANT, respectively, was generated by oligonucleotide-directed mutagenesis. pCMV-FL-CAV2, encoding FLAG-tagged CAV2, was prepared by inserting the PCR product amplified with 5′-GTTGTCGACTATGGGGCTGGAGAC-3′ and 5′-GTTAAGCTTTCAATCCTGGCTC-3′ as primers and human liver cDNA library (Clontech) as a template into the SalI-HindIII site of pCMV-FLAG vector (21). The mammalian expression vector for the C domain of ESRα was generated by replacing the EcoRI-XhoI digestion of pCMV-FLAG vector (21) by that of pGEX-ESRα C. pLMH14 was described previously (26). pGL3-EREX3-TATA-Luc, pcDNA3-ERα, pcDNA3-hERβ were kindly provided by Dr. Kato (Institute of Molecular and Cellular Biosciences, University of Tokyo). JFH1 expression plasmid was provided by Dr. Wakita (National Institute of Infectious Diseases).

Luciferase Assay—A luciferase assay monitoring HCV replication activity was performed as described previously (22, 26). In Fig. 1, *A* and *F*, we used LucNeo#2 cells, stably carrying luciferase-containing subgenomic replicon (22). In Figs. 2 (*D* and *E*), 4*C*, and 6*A*, we transiently transduced luciferase-containing replicon LMH14 RNA together with each expression plasmid into cured MH-14 cells (26). A luciferase assay detecting the transcriptional activity driven from the ERE was performed as described previously (25).

Real Time RT-PCR Analysis—Real time RT-PCR analysis was performed as previously described (20).

Immunoblot Analysis—Immunoblot analysis was performed as previously described (25). The antibodies used in this study are anti-NS5A (kindly provided by Dr. Takamizawa (Osaka University)), anti-NS5B (anti-NS5B#14; a generous gift from Dr. Kohara (Tokyo Metropolitan Institute of Medical Science)), anti-NS5B (NS5B#6; a kind gift from Dr. Fukuya (Osaka University)), anti-tubulin (Oncogene), anti-FLAG (Sigma), anti-IκBα (Santa Cruz Biotechnology, Inc., Santa Cruz, CA), anti-calnexin (StressGen), and anti-caveolin-2 antibodies (BD Biosciences Pharmingen).

Indirect Immunofluorescence Analysis—Indirect immunofluorescence analysis was performed as described previously (25). The antibodies used were anti-NS5A and anti-protein-disulfide isomerase antibodies (StressGen).

siRNA—siRNA duplexes (5′-GUGUGCAAUGACUAUGCUUCA-3′ for si-ESRα and 5′-CGCAUCGGGAUAUCACUAUGG-3′ for si-ESRβ) were synthesized (Proligo). A randomized siRNA, si-control, was purchased from Dharmacon (nonspecific control duplex IX).

Enzyme-linked Immunosorbent Assay—HCV core was quantified in the culture medium of the cells transfected with JFH1 RNA (29) with an enzyme-linked immunosorbent assay according to the manufacturer's protocol (HCV antigen enzyme-linked immunosorbent assay test; Ortho-Clinical Diagnostics).

RT-PCR Analysis—RT-PCR analysis was performed as described (20) by using the following primer sets: 5′-CCTACTACCTGGAGAACG-3′ and 5′-GCTGGACACATATAGTCG-3′ for the detection of ESRα and 5′-AGCCATGACATTCTATAGC-3′ and 5′-CCACTTCGTAACACTTCC-3′ for ESRβ.

GST Pull-down Assay—The GST pull-down assay was conducted as described previously (25).

Immunoprecipitation Analysis—Immunoprecipitation analysis was performed as described previously (25). The antibodies

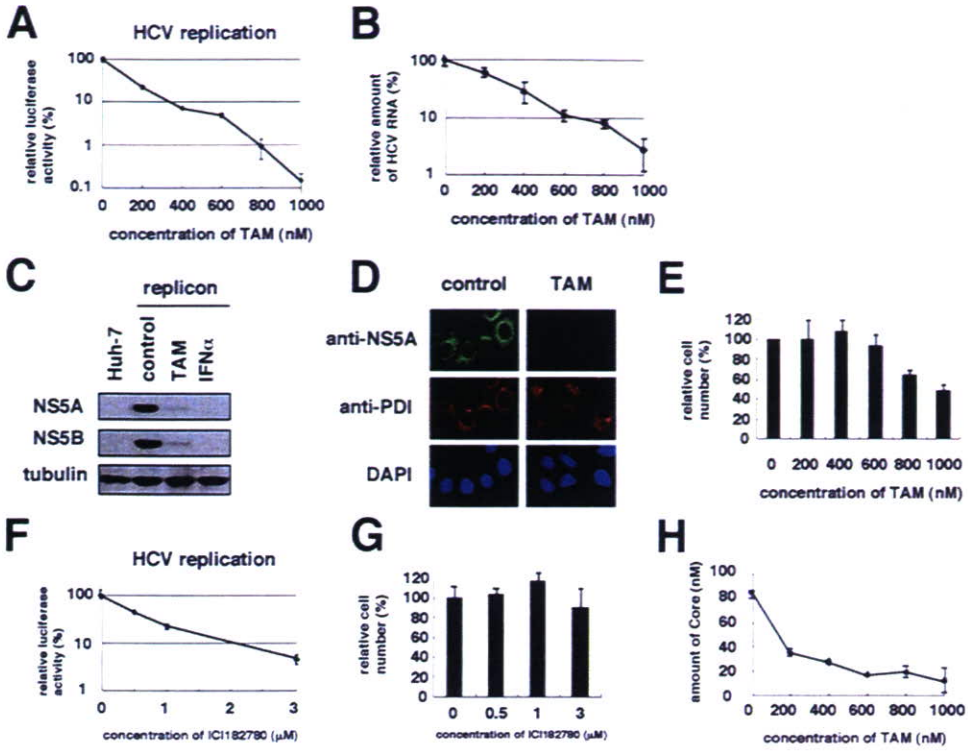

FIGURE 1. **TAM suppressed the replication of the HCV genome.** *A*, luciferase activities were measured using the LucNeo#2 cells, which carried a luciferase-containing replicon RNA, upon treatment with TAM at the indicated doses for 7 days. Relative luciferase activities are plotted against the concentrations of TAM. The data show the means of three independent experiments. The *error bars* are indicated. *B*, HCV RNA was quantified by real time RT-PCR analysis using the lysates from MH-14 cells, harboring the HCV subgenomic replicon, treated with the indicated doses of TAM for 7 days. Relative amounts of HCV RNA are shown. *C*, HCV NS5A and NS5B proteins as well as tubulin as an internal control were detected by immunoblot analysis in the lysates from MH-14 cells (replicon) treated without (control) or with 500 nM TAM or 100 IU/ml interferon-α as a positive control for 7 days and Huh-7 cells. *D*, HCV NS5A and protein-disulfide isomerase (*PDI*) as an internal control were detected by indirect immunofluorescence analysis in the cells treated without (control) or with 500 nM TAM for 7 days. 4′,6-Diamidino-2-phenylindole (*DAPI*) shows a nuclear staining. *E*, cell number was counted after 5 days upon treatment with various concentrations of TAM. Relative cell numbers are shown. *F*, luciferase activities with LucNeo#2 cells treated with various concentrations of ICI182780 were measured as described in *A*. *G*, cell number was counted under treatment with ICI182780 at the indicated concentrations. *H*, core in the culture medium of JFH1 RNA-transfected cells upon treatment with TAM was quantified as described under "Experimental Procedures."

used in this study were mouse normal IgG as a negative control (Zymed Laboratories), anti-NS5B (anti-NS5B#10; a generous gift from Dr. Kohara at the Tokyo Metropolitan Institute of Medical Science), anti-FLAG, and anti-caveolin-2 antibodies.

Fractionation of Cell Extracts—MH-14 cells transfected with the expression plasmid for FLAG-tagged ESRα were fractionated essentially as described previously (25).

HCV Replication Complex Assay—Isolation of HCV RC was done as described previously (16, 21).

In Vitro HCV Infection Experiment—*In vitro* HCV infection was conducted essentially as described (23). Briefly, HCV-infected serum (~2×10^5 copies) was inoculated into HuS-E7/DN24 cells (5×10^4 cells) for 24 h. After washes, cells were cultured in the medium supplemented with 10 μM PD98059 to stimulate HCV translation (27) (*scheme* in Fig. 6*B*). To observe HCV amplification, HCV RNA in the cells was quantified, since HCV RNA was hardly detected significantly in the culture medium (23).

3-(4,5-Dimethylthiazol-2-yl)-2,5-diphenyltetrazolium bromide Assay—The 3-(4,5-dimethylthiazol-2-yl)-2,5-diphenyltetrazolium bromide assay was performed to examine the cell viability using Cell Proliferation kit II, XTT (Roche Applied Science) according to the manufacturer's protocol.

RESULTS

Tamoxifen Suppressed HCV Genome Replication—We screened for agents that suppressed HCV genome replication using a HCV subgenomic replicon system (13, 16). Among the compounds tested, we observed that TAM inhibited HCV genome replication. HCV replication activity, monitored by luciferase activity (22), and the amount of HCV RNA were decreased with TAM treatment in a dose-dependent manner (Fig. 1, *A* and *B*). The expression of HCV proteins, NS5A and NS5B, detected by immunoblot (Fig. 1*C*) and indirect immuofluorescence analyses (Fig. 1*D*), also drastically decreased by treatment with TAM. A high concentration of TAM decreased cell proliferation (Fig. 1*E*). However, TAM suppressed HCV replication without any cytotoxicity in another cell line, HuS-E7/DN24 cells (Fig. 6, *C* and *D*). In addition, a pure anti-estrogen compound ICI182780, which had little cytotoxic effect, reduced HCV RNA (Fig. 1, *F* and *G*). Moreover, TAM inhibited the production of core in the culture medium of HCV JFH1-transfected cells, in a recently developed system of the production of infectious HCV particles (Fig. 1*H*) (28–30). The above data indicate that TAM suppresses HCV genome replication.

ESR Was Involved in HCV Genome Replication—Next, we investigated which cellular protein TAM targets to suppress HCV replication. It has been reported that TAM targets 1) ESR (31), 2) P-glycoprotein (32, 33), 3) calmodulin (34), 4) protein kinase C (35, 36), etc. Although other compounds targeting P-glycoprotein, calmodulin, and protein kinase C did not affect HCV replication in our screening (data not shown), ESR was suggested to play a role in HCV replication as shown below.

RNAi-mediated specific knockdown of endogenous ESRα and ESRβ (Fig. 2*A*) reduced HCV RNA in replicon-containing cells to ~20–40% and 60–70%, respectively (Fig. 2*B*). Transient transfection with ESRα and ESRβ expression plasmids, which activated ERE-driven transcription 4–5-fold (Fig. 2*C*), showed that ectopically expressed ESRα augmented HCV replication activity in a dose-dependent manner, whereas ESRβ did not (Fig. 2*D*). ESRα-induced augmentation of the replication was reversed upon TAM treatment (Fig. 2*D*). These results suggested a significant role of ESR, especially ESRα, in HCV

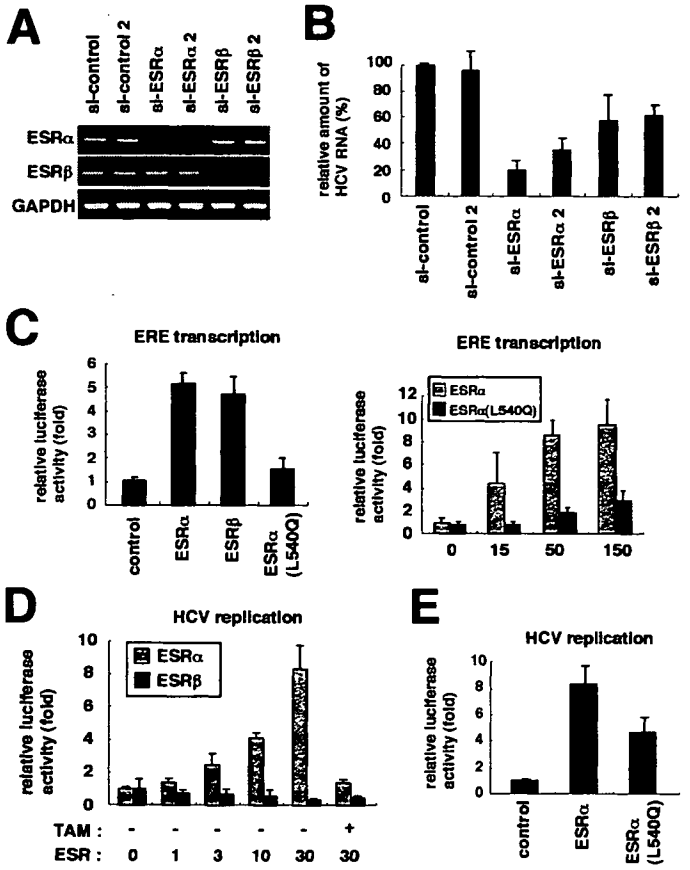

FIGURE 2. **ESR was involved in HCV genome replication.** *A*, specific knockdown of endogenous ESRα and ESRβ. RT-PCR analysis was performed to detect the expression of ESRα, ESRβ, and glyceraldehyde-3-phosphate dehydrogenase (*GAPDH*) as an internal control in the cells transfected with siRNA recognizing ESRα (si-ESRα, si-ESRα2), ESRβ (si-ESRβ, si-ESRβ2), or randomized siRNA (si-control, si-control2). *B*, HCV RNA was quantified as shown in Fig. 1*B*, using the cells transfected with si-control, si-control2, si-ESRα, si-ESRα2, si-ESRβ, and si-ESRβ2 for 5 days. *C*, the ERE-mediated transcriptional activities were measured by a luciferase assay using the lysates from the cells transfected with pGL3-EREX3-TATA-Luc reporter plasmid together with pcDNA3-ERα (ESRα), pcDNA3-hERβ (ESRβ), pcDNA-ESRα(L540Q), or the empty vector (control) (*left*) or varying amounts (ng) of pcDNA3-ERα (ESRα) or pcDNA-ESRα(L540Q) (*right*) and treated with 100 nM estradiol for 36 h. *D* and *E*, HCV replication activities were examined by quantifying the luciferase activities using cured MH-14 cells transfected with the indicated doses (ng) of ESRα or ESRβ (*D*) or 30 ng of ESRα, ERα(L540Q), or the empty vector (control) (*E*) together with 0.125 μg of LMH14 RNA without or with 1 μM TAM for 4 days.

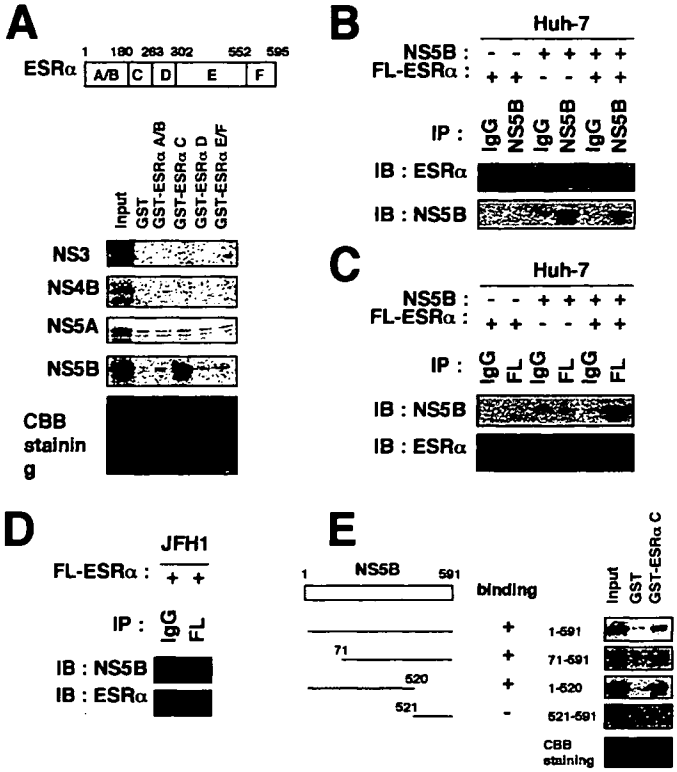

FIGURE 3. **ESRα interacted with HCV NS5B.** *A*, *top*, schematic representation of the primary structure of ESRα. ESRα consists of domains A–F. The amino acid numbers are also shown. *Bottom*, GST pull-down assays were performed using the recombinant proteins of the A/B, C, D, and E/F domain of ESRα fused with GST and *in vitro* translated HCV NS3, NS4B, NS5A, and NS5B protein. *Input*, the one-fifth amount of protein used for the pull-down assay. The Coomassie Brilliant Blue staining pattern of the precipitated fraction is also shown in the *bottom panel*. *B–D*, the lysates from the cells ectopically expressing NS5B (*B* and *C*) or the whole open reading frame of the HCV JFH1 strain (*D*) and/or FLAG-tagged ESRα were immunoprecipitated (*IP*) with anti-NS5B (*B*; NS5B), anti-FLAG antibody (*C* and *D*; FL), or mouse normal IgG as a negative control followed by the detection of ESRα and NS5B by immunoblot analysis (*IB*). *E*, deletion mutants of NS5B were subjected to a GST pull-down assay with GST-fused C domain of ESRα as described in *A*. The *left panel* shows a schematic representation of the full-length and truncated mutants of NS5B. The *numbers* indicate the amino acid numbers in NS5B.

genome replication. ESRα(L540Q), carrying a leucine to glutamine point mutation at aa 540 within the L*XX*LL motif (aa 536–540) of ESRα (37), had much lower transactivation activity driven from ERE (Fig. 2*C*). However, ESRα(L540Q) stimulated HCV replication activity ~5-fold, although the stimulation was less than that by wild-type ESRα (Fig. 2*E*). Thus, ESRα having lower transactivating capacity could still facilitate HCV replication.

ESRα Interacted with HCV NS5B—Thus, the chemical biology approach revealed the involvement of ESR in HCV genome replication. Then we investigated the molecular mechanism of ESR-induced HCV replication. A binding assay between ESRα and HCV proteins expressed in the HCV subgenomic replicon showed that the C domain of ESRα coprecipitated with NS5B but not NS3, NS4B, and NS5A (Fig. 3*A*). Other ESRα domains, A/B, D, and E/F, did not bind to any HCV proteins. A coimmunoprecipitation assay also indicated the presence of ESRα in the immunoprecipitate by anti-NS5B antibody (Fig. 3, *B* and *D*), and *vice versa* (Fig. 3*C*). Thus, ESRα specifically interacted with NS5B. Deletion analysis indicated that the region of 71–591 and 1–520 but not 521–591 of NS5B coprecipitated with the recombinant C domain of ESRα (Fig. 3*E*). This binding profile is different from that between cyclophilin B and NS5B, which we previously reported (21).

The ESRα-NS5B Interaction Was Important for the Regulation of HCV Genome Replication—To examine whether the interaction between ESRα and NS5B was essential for the ESRα-mediated regulation of HCV replication or not, we searched for a point mutant of ESRα that could not bind to NS5B by alanine-scanning mutation analysis. ESRα mutants, ESRα(255M) and ESRα(258M), in which IRK at aa 255–257 and DRR at aa 258–260 was replaced by TGT and AQT, respectively, had little affinity with NS5B (Fig. 4*A*) but still possessed the ERE-mediated transactivation capacity (Fig. 4*B*). However, both ESRα(255M) and ESRα(258M) caused only weak activations of HCV replication, compared with wild type ESRα (Fig. 4*C*). The data suggest that the interaction of ESRα with NS5B is

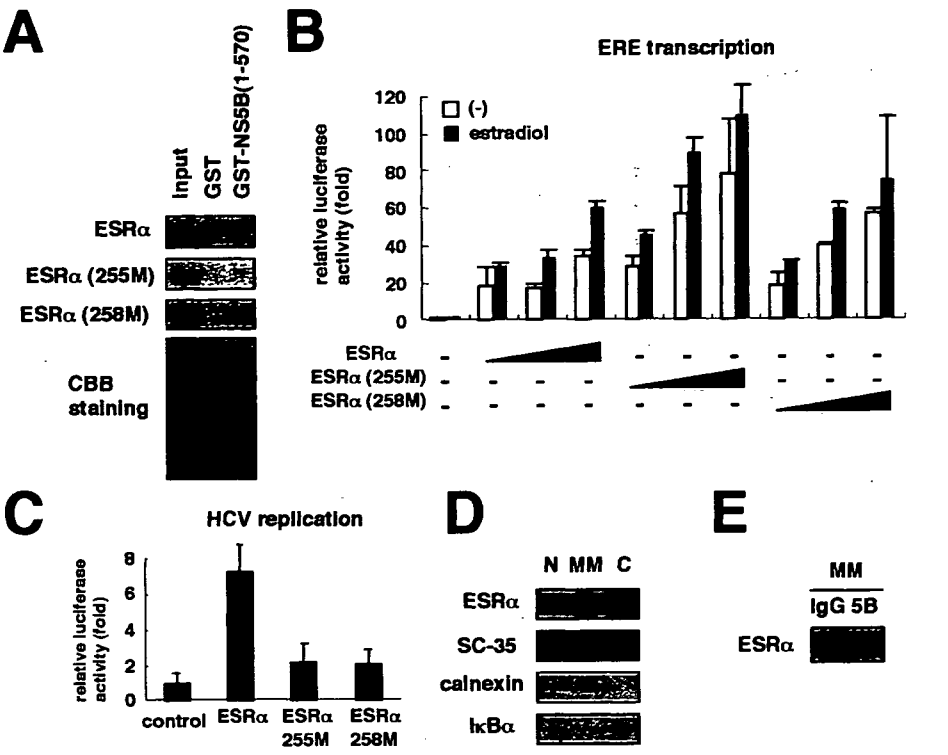

FIGURE 4. **The interaction of NS5B mediated the regulation of HCV genome replication by ESRα.** *A*, GST pull-down assays were performed as described in Fig. 3*A* using the wild type ESRα or point mutant of ESRα, ESRα(255M), and ESRα(258M). *B*, the mutation within ESRα(255M) and ESRα(258M) did not reduce the activation capacity of ERE-mediated transcription. Huh-7 cells were transfected with the expression plasmids for ESRα, ESRα(255M), or ESRα(258M) at doses of 10, 30, and 100 ng each together with pGL3-EREX3-TATA-Luc reporter plasmid and treated without (*white bar*) or with 100 nM estradiol (*black bar*) to quantify the luciferase activity. *C*, HCV replication activities were examined by quantifying the luciferase activities as described in the legend to Fig. 2*D* in the cells upon transfection with the expression plasmids for wild type ESRα, ESRα(255M), or ESRα(258M). *D*, the cells were fractionated into the nucleus (*N*), MM, and cytoplasm (*C*). Each fraction was detected for FLAG-tagged ESRα, SC-35, calnexin, and IκBα, respectively, by immunoblot analysis. Calnexin, an ER marker protein, was detected in the nucleus as well as MM, probably because of the existence of the nuclear membrane in the nuclear fraction. *E*, the MM fraction obtained in *D* was subjected to a coimmunoprecipitation assay using anti-NS5B or IgG followed by immunoblot analysis for the detection for ESRα.

critical for ESRα-mediated regulation of HCV genome replication.

Thus, ESRα interaction with NS5B regulates HCV replication. NS5B is mainly located on the cytoplasmic surface of the ER membrane (21, 38). On the other hand, ESRα as a nuclear hormone receptor is normally distributed in the cytoplasm and translocates into the nucleus upon ligand stimulation. In addition, a part of ESRα localizes on the membrane fraction. In our experiment, NS5B was mainly located around the ER, colocalized with the ER marker, protein-disulfide isomerase (data not shown) (21). Ectopically expressed ESRα showed diffuse distribution in the cells (data not shown). We fractionated cell homogenates and observed that a part of the ESRα resided in the microsomal membrane (MM) fraction (Fig. 4*D*). Moreover, ESRα in the MM fraction was coprecipitated with NS5B (Fig. 4*E*). It suggests the possibility that the interaction between NS5B and ESRα, at least in part of them, occurs on the ER membrane.

ESRα Promoted the Participation of NS5B in the HCV Replication Complex—It was reported that HCV proteins involved in the replication machinery was associated with the lipid raft on the ER and cofractionated with CAV2. A coimmunoprecipitation assay showed that NS5B associated with CAV2 (Fig. 5*A*). In the experiment investigating the role of ESRα in NS5B-CAV2 association, the coprecipitation of NS5B with CAV2 was decreased upon the knocking down of ESRα (Fig. 5*B*). Treatment with TAM abrogated the association of NS5B with CAV2 (Fig. 5*C*), although the total amount of NS5B in the cells is similar in the presence and absence of TAM for 24 h in this experiment (data not shown). Thus, ESRα was suggested to promote the association between NS5B and CAV2. Since a part of CAV2 resided on the lipid raft on the ER (18), ESRα-mediated binding between NS5B and CAV2 was possible to affect the localization of NS5B to the HCV RC. To see the consequential relevance of ESRα on NS5B function, we analyzed the HCV RC by treatment with digitonin/protease as described previously (16). HCV proteins involved in the RC and surrounded by the membrane structure are resistant to the treatment with digitonin followed by protease, whereas those unrelated to the replication outside the RC are digested by the treatment. By using this technique measuring the sensitivity to protease, HCV RC can be distinguished from the ER that is not related to the replication, although the RC and the nucleus cannot be separated. The experimental condition for fractionation was confirmed with the detection with IκBα and calnexin; a cytosolic protein IκBα was washed out following the treatment with digotinin (Fig. 5*D*, *lanes 1* and *2*), and ER protein calnexin, which did not accumulate in the RC, was digested by treatment with digotinin/protease (Fig. 5*D*, *lanes 2–4*). An ER lipid raft component, CAV2, was still detected under the digitonin/protease treatment (the RC-containing fraction) (Fig. 5*D*, *lanes 3* and *4*). Under this condition, a part of NS5B was detected in the digitonin/protease-resistant fraction, as described previously (16) (Fig. 5*D*, *lanes 3* and *4*). However, NS5B in this fraction was decreased upon treatment with TAM (Fig. 5*D*, *lanes 3*, *4*, *7*, and *8*). On the other hand, the amount of NS5A was not significantly changed by TAM treatment. Knocking down of ESRα also disrupted the association of NS5B with the RC-containing fraction (Fig. 5*E*). From the above results, it was suggested that ESRα promoted the participation of NS5B in the RC (also see "Discussion").

ESRα Could Serve as a Molecular Target of Anti-HCV Agents—Finally, we assessed the possibility that the association of ESRα with NS5B could serve as a target of anti-HCV agents. By introducing a decoy peptide against ESRα-NS5B interaction, consisting of the C domain of ESRα into replicon-bearing cells,

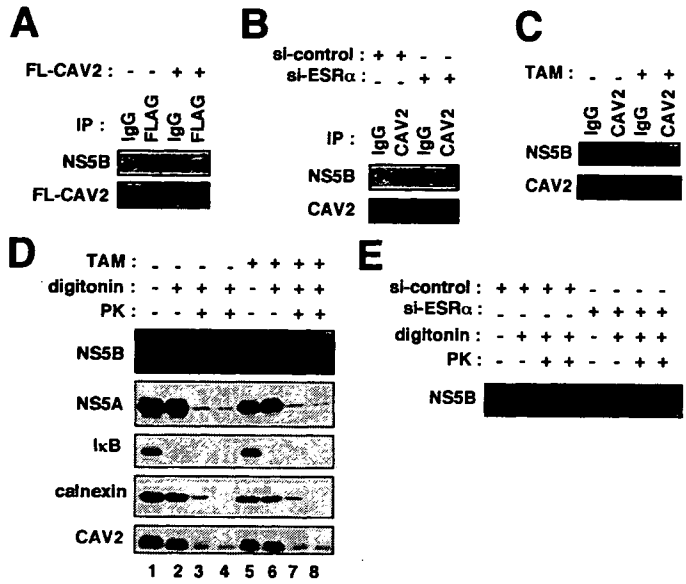

FIGURE 5. **ESRα promoted the participation of NS5B in HCV RC.** *A–C*, a coimmunoprecipitation assay (*IP*) was performed with anti-FLAG (*A*), anti-CAV2 (*B* and *C*) antibody, or mouse normal IgG from the lysates of the cells transfected without or with FLAG-tagged CAV2 (*A*), transfected with si-control or si-ESRα (*B*), or treated without or with 1 μM TAM (*C*). NS5B (*top*) and CAV2 (*bottom*) were detected by immunoblot analysis. *D*, detection of the amount of NS5B in the digitonin/protease-resistant fraction. MH-14 cells were treated without (*lanes 1–4*) or with 1 μM TAM (*lanes 5–8*) for 24 h. Cells were then treated without (*lanes 1* and *5*) or with digitonin (*lanes 2–4* and *6–8*), followed by digestion with proteinase K (0 μg/ml for *lanes 2* and *6*, 0.3 μg/ml for *lanes 3* and *7*, and 1 μg/ml for *lanes 4* and *8*). NS5B, NS5A, IκBα, calnexin, and CAV2 were detected by immunoblot analysis. *E*, HCV RC was isolated as described in *D* using the cells transfected with si-control or si-ESRα, and NS5B was detected. A similar result was obtained by using si-ESRα2.

HCV replication activity was reduced in a dose-dependent manner (Fig. 6*A*). To further observe the significance of ESRα in a physiological condition, we performed an *in vitro* infection experiment using serum from an HCV-infected patient as a nascent virus inoculum and nonneoplastic human hepatocytes as highly infection-permissive cells (Fig. 6*B*). Treatment with 1 μM TAM did not show a cytotoxic effect on these cells in any time course examined (Fig. 6*C*). However, treatment with TAM as well as cyclosporin A as a positive control inhibited the multiplication of viral genome RNA in the cells along with the time course (Fig. 6*D*). Thus, ESRα could serve as a potent molecular target of anti-HCV agents.

DISCUSSION

In general, viruses take advantage of host cell factors for their replication. So far, some factors have been shown to relevantly regulate HCV replication, including hVAP33 (39, 40), FBL2 (41), and cyclophilin B (21). Among these, FBL2 and cyclophilin B were identified by a chemical biological approach; FBL2 from the observation of an anti-HCV activity of lovastatin and an inhibitor of geranylgeranyl transferase (41–43); cyclophilin B from the inhibitory effect of cyclosporin A on HCV replication (20, 21). In this study, we found a suppressive capacity of TAM to HCV genome replication. Through further examination using TAM, we revealed ESRα as a host cell factor regulating HCV replication and suggested its regulation mechanism.

Currently, it is proposed that HCV RC that replicates the HCV genome is formed on the intracellular membrane, including the ER membrane (14–17). It was also reported that HCV genome replication was associated with the lipid raft on the intracellular membrane (18). Most HCV proteins are not related to the RC, whereas only a minor portion of HCV proteins take part in the RC to drive the viral replication (16). It has remained widely unknown, however, how HCV proteins are regulated to participate in the RC. It was reported that hVAP-33 binds to NS5A and NS5B, and this protein is related to the amount of NS5B in the lipid raft (40). hVAP-33 was speculated to recruit NS5B to the lipid raft, although its molecular mechanism has not been analyzed. This study suggested the interaction between ESRα and NS5B in the ER fraction, although we did not show the existence of ESRα in the RC, since the RC and the nucleus cannot be separated in the digitonin/protease treatment experiment. ESRα promoted the interaction of NS5B with CAV2. Previous papers reported that ESRα bound to CAV1 and CAV2 (6). From these observations, ESRα is

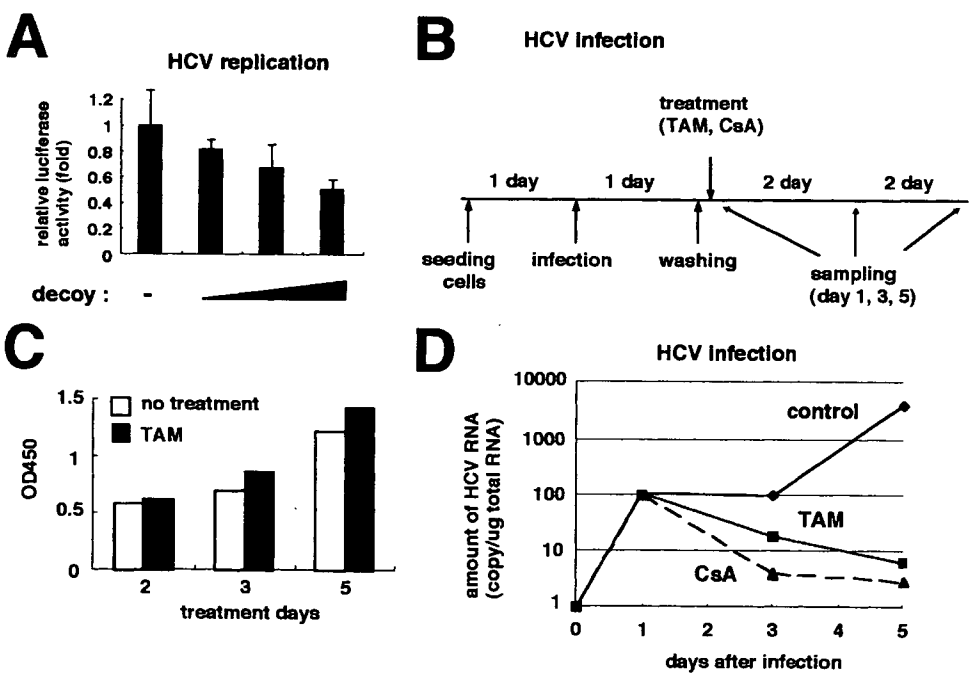

FIGURE 6. **ESRα could serve as a molecular target for anti-HCV agents.** *A*, HCV replication activity was measured by quantifying the luciferase activity as described in the legend to Fig. 2*D* in the cells overexpressing a decoy peptide consisting of the C domain of ESRα. *B*, experimental scheme of *in vitro* HCV infection experiment. After seeding the HuS-E7/DN24 cells, HCV-positive serum was inoculated for 24 h. After extensive washes, the cells were cultured with the medium supplemented without (control) or with 1 μM TAM or 3 μg/ml cyclosporin A. HCV genome RNA was quantified along with the time course (days 1, 3, and 5 postinoculation) by real time RT-PCR analysis. *C*, the treatment with 1 μM TAM did not show any cytotoxic effect on HuS-E7/DN24 cells. 3-(4,5-Dimethylthiazol-2-yl)-2,5-diphenyltetrazolium bromide assays were performed as described under "Experimental Procedures" to examine the viability of the cells at days 2, 3, and 5 postinoculation. *D*, HCV genome RNA was quantified as described in *B* and plotted against the time course.

likely to function as a bridging factor that connects NS5B to CAV2, although we cannot fully neglect the possibility that ESRα augments NS5B-CAV2 binding via another function, such as transcriptional activity. Because CAV2 resided on the lipid raft of the intracellular membrane (18), this action of ESRα may recruit NS5B to the lipid raft and the HCV RC. In fact, ESRα promoted the participation of NS5B in the HCV RC. Thus, ESRα is suggested to escort NS5B to the HCV RC, although it is also possible that ESRα augments the number of the RC itself. However, ESRα at least augments the amount of NS5B involved in HCV replication machinery to stimulate the replication. It was reported that the membrane-associated ESRα served as a platform where signalsomes, including receptor tyrosine kinase, nonreceptor tyrosine kinase Src, and G proteins, assembled and activated downstream signaling pathways (44–46). HCV may also take advantage of such platform characteristics of ESRα to form the RC for their efficient replication. Although the mechanisms of the nuclear receptor function of ESRα have been extensively elucidated, the functions of membrane-associated ESRα have not been widely characterized so far. This study suggested a novel physiological relevance of membrane-associated ESRα as a regulator of the viral replication.

Until now, there are no clinical studies that report a direct interaction of TAM treatment with HCV replication in patients infected with HCV. Given our results, examinations on the effect of TAM or other anti-estrogen drugs may be one of the useful approaches to develop a new anti-HCV strategy. On the other hand, we disclosed the mechanism of ESR-mediated regulation of HCV genome replication. Screening for compounds that inhibit this mechanism expectedly led to novel types of anti-HCV agents. Further analyses on ESR are needed to develop anti-HCV therapeutics as well as reveal the regulation mechanism of HCV replication.

Acknowledgments—We are grateful to Dr. T. Murata, T. Hishiki, and M. Hosaka for establishing the replicon-containing cells. We thank Dr. Aratake (Asahi Kasei Pharma) for helpful discussions. We also thank Dr. Kato, Dr. Takamizawa, Dr. Kohara, Dr. Fukuya, and Dr. Wakita for kindly providing the plasmids: pGL3-EREX3-TATA-Luc, pcDNA3-ERα, and pcDNA3-hERβ; anti-NS5A antibody; anti-NS5B antibody; anti-NS5B antibody; and JFH1 expression plasmid, respectively.

REFERENCES

1. Mangelsdorf, D. J., Thummel, C., Beato, M., Herrlich, P., Schutz, G., Umesono, K., Blumberg, B., Kastner, P., Mark, M., Chambon, P., and Evans, R. M. (1995) *Cell* **83,** 835–839
2. Acconcia, F., and Kumar, R. (2006) *Cancer Lett.* **238,** 1–14
3. Levin, E. R. (2005) *Mol. Endocrinol.* **19,** 1951–1959
4. Song, R. X., Zhang, Z., and Santen, R. J. (2005) *Trends Endocrinol. Metab.* **16,** 347–353
5. Razandi, M., Alton, G., Pedram, A., Ghonshani, S., Webb, P., and Levin, E. R. (2003) *Mol. Cell. Biol.* **23,** 1633–1646
6. Razandi, M., Oh, P., Pedram, A., Schnitzer, J., and Levin, E. R. (2002) *Mol. Endocrinol.* **16,** 100–115
7. Marquez, D. C., Chen, H. W., Curran, E. M., Welshons, W. V., and Pietras, R. J. (2006) *Mol. Cell. Endocrinol.* **246,** 91–100
8. Liang, T. J., Jeffers, L. J., Reddy, K. R., De Medina, M., Parker, I. T., Cheinquer, H., Idrovo, V., Rabassa, A., and Schiff, E. R. (1993) *Hepatology* **18,** 1326–1333
9. Grakoui, A., Wychowski, C., Lin, C., Feinstone, S. M., and Rice, C. M. (1993) *J. Virol.* **67,** 1385–1395
10. Hijikata, M., Kato, N., Ootsuyama, Y., Nakagawa, M., and Shimotohno, K. (1991) *Proc. Natl. Acad. Sci. U. S. A.* **88,** 5547–5551
11. Bartenschlager, R., and Lohmann, V. (2001) *Antiviral Res.* **52,** 1–17
12. Tellinghuisen, T. L., and Rice, C. M. (2002) *Curr. Opin. Microbiol.* **5,** 419–427
13. Lohmann, V., Korner, F., Koch, J., Herian, U., Theilmann, L., and Bartenschlager, R. (1999) *Science* **285,** 110–113
14. Aizaki, H., Lee, K. J., Sung, V. M., Ishiko, H., and Lai, M. M. (2004) *Virology* **324,** 450–461
15. Egger, D., Wolk, B., Gosert, R., Bianchi, L., Blum, H. E., Moradpour, D., and Bienz, K. (2002) *J. Virol.* **76,** 5974–5984
16. Miyanari, Y., Hijikata, M., Yamaji, M., Hosaka, M., Takahashi, H., and Shimotohno, K. (2003) *J. Biol. Chem.* **278,** 50301–50308
17. Moradpour, D., Gosert, R., Egger, D., Penin, F., Blum, H. E., and Bienz, K. (2003) *Antiviral Res.* **60,** 103–109
18. Shi, S. T., Lee, K. J., Aizaki, H., Hwang, S. B., and Lai, M. M. (2003) *J. Virol.* **77,** 4160–4168
19. Watashi, K., and Shimotohno, K. (2007) *Rev. Med. Virol.* **17,** 245–252
20. Watashi, K., Hijikata, M., Hosaka, M., Yamaji, M., and Shimotohno, K. (2003) *Hepatology* **38,** 1282–1288
21. Watashi, K., Ishii, N., Hijikata, M., Inoue, D., Murata, T., Miyanari, Y., and Shimotohno, K. (2005) *Mol. Cell* **19,** 111–122
22. Goto, K., Watashi, K., Murata, T., Hishiki, T., Hijikata, M., and Shimotohno, K. (2006) *Biochem. Biophys. Res. Commun.* **343,** 879–884
23. Aly, H. H., Watashi, K., Hijikata, M., Kaneko, H., Takada, Y., Egawa, H., Uemoto, S., and Shimotohno, K. (2007) *J. Hepatol.* **46,** 26–36
24. Hino, H., Tateno, C., Sato, H., Yamasaki, C., Katayama, S., Kohashi, T., Aratani, A., Asahara, T., Dohi, K., and Yoshizato, K. (1999) *Biochem. Biophys. Res. Commun.* **256,** 184–191
25. Watashi, K., Hijikata, M., Tagawa, A., Doi, T., Marusawa, H., and Shimotohno, K. (2003) *Mol. Cell. Biol.* **23,** 7498–7509
26. Murata, T., Ohshima, T., Yamaji, M., Hosaka, M., Miyanari, Y., Hijikata, M., and Shimotohno, K. (2005) *Virology* **331,** 407–417
27. Murata, T., Hijikata, M., and Shimotohno, K. (2005) *Virology* **340,** 105–115
28. Lindenbach, B. D., Evans, M. J., Syder, A. J., Wolk, B., Tellinghuisen, T. L., Liu, C. C., Maruyama, T., Hynes, R. O., Burton, D. R., McKeating, J. A., and Rice, C. M. (2005) *Science* **309,** 623–626
29. Wakita, T., Pietschmann, T., Kato, T., Date, T., Miyamoto, M., Zhao, Z., Murthy, K., Habermann, A., Krausslich, H. G., Mizokami, M., Bartenschlager, R., and Liang, T. J. (2005) *Nat. Med.* **11,** 791–796
30. Zhong, J., Gastaminza, P., Cheng, G., Kapadia, S., Kato, T., Burton, D. R., Wieland, S. F., Uprichard, S. L., Wakita, T., and Chisari, F. V. (2005) *Proc. Natl. Acad. Sci. U. S. A.* **102,** 9294–9299
31. Shang, Y. (2006) *Nat. Rev. Cancer* **6,** 360–368
32. Callaghan, R., and Higgins, C. F. (1995) *Br. J. Cancer* **71,** 294–299
33. Raderer, M., and Scheithauer, W. (1993) *Cancer* **72,** 3553–3563
34. Lopes, M. C., Vale, M. G., and Carvalho, A. P. (1990) *Cancer Res.* **50,** 2753–2758
35. O'Brian, C. A., Liskamp, R. M., Solomon, D. H., and Weinstein, I. B. (1985) *Cancer Res.* **45,** 2462–2465
36. O'Brian, C. A., Ward, N. E., and Anderson, B. W. (1988) *J. Natl. Cancer Inst.* **80,** 1628–1633
37. Leers, J., Treuter, E., and Gustafsson, J. A. (1998) *Mol. Cell. Biol.* **18,** 6001–6013
38. Schmidt-Mende, J., Bieck, E., Hugle, T., Penin, F., Rice, C. M., Blum, H. E., and Moradpour, D. (2001) *J. Biol. Chem.* **276,** 44052–44063
39. Evans, M. J., Rice, C. M., and Goff, S. P. (2004) *Proc. Natl. Acad. Sci. U. S. A.* **101,** 13038–13043
40. Gao, L., Aizaki, H., He, J. W., and Lai, M. M. (2004) *J. Virol.* **78,** 3480–3488
41. Wang, C., Gale, M., Jr., Keller, B. C., Huang, H., Brown, M. S., Goldstein, J. L., and Ye, J. (2005) *Mol. Cell* **18,** 425–434

42. Kapadia, S. B., and Chisari, F. V. (2005) *Proc. Natl. Acad. Sci. U. S. A.* **102,** 2561–2566
43. Ye, J., Wang, C., Sumpter, R., Jr., Brown, M. S., Goldstein, J. L., and Gale, M., Jr. (2003) *Proc. Natl. Acad. Sci. U. S. A.* **100,** 15865–15870
44. Migliaccio, A., Piccolo, D., Castoria, G., Di Domenico, M., Bilancio, A., Lombardi, M., Gong, W., Beato, M., and Auricchio, F. (1998) *EMBO J.* **17,** 2008–2018
45. Razandi, M., Pedram, A., Greene, G. L., and Levin, E. R. (1999) *Mol. Endocrinol.* **13,** 307–319
46. Wyckoff, M. H., Chambliss, K. L., Mineo, C., Yuhanna, I. S., Mendelsohn, M. E., Mumby, S. M., and Shaul, P. W. (2001) *J. Biol. Chem.* **276,** 27071–27076

Gene Therapy (2008), 1–11

www.nature.com/gt

ORIGINAL ARTICLE

Inhibition of tumor cell growth in the liver by RNA interference-mediated suppression of HIF-1α expression in tumor cells and hepatocytes

Y Takahashi, M Nishikawa and Y Takakura
Department of Biopharmaceutics and Drug Metabolism, Graduate School of Pharmaceutical Sciences, Kyoto University, Kyoto, Japan

Hypoxia-inducible factor-1 (HIF-1) is a ubiquitously expressed oxygen-regulated transcription factor composed of α and β subunits. HIF-1 activates transcription of various genes including those involved in metastatic tumor growth. In the present study, HIF-1α expression in tumor-bearing mouse liver was examined after inoculation of tumor cells into portal vein. We found that tumor-bearing liver showed greatly increased HIF-1α expression. Plasmid DNA (pDNA) expressing short hairpin RNA targeting HIF-1α (pshHIF-1α) was effective in suppressing protein expression of HIF-1α in vitro. *Intravenous injection of pshHIF-1α by hydrodynamics-based procedure reduced the HIF-1α protein expression in both normal and tumor cells and tumor cell number in the liver. Pre-injection of pshHIF-1α to mice, by which pDNA was delivered only to liver cells, not to tumor cells, was also effective in reducing the number of tumor cells inoculated 3 days after pDNA injection. These findings indicate that HIF-1α expression is increased in normal liver cells as well as tumor cells, and HIF-1α expression plays an important role in tumor progression. Use of the RNA interference (RNAi) of HIF-1 is an effective strategy for inhibiting tumor cell growth, and both tumor and normal cells can be the target for RNAi-based anticancer treatment.*
Gene Therapy advance online publication, 14 February 2008; doi:10.1038/sj.gt.3303103

Keywords: *RNAi; HIF-1α; gene delivery; hydrodynamics-based procedure; hepatic metastasis*

Introduction

Metastasis, which is the transfer of cancer cells from one organ to other organs, is the most distinctive feature of malignant tumors and is the cause of approximately 90% of human cancer deaths.[1,2] Tumor metastasis is an exceedingly complex process, which occurs through a series of sequential steps that include dissociation from the primary tumor, invasion of adjacent tissues, intravasation, transport through the circulatory system, arrest in small vessels, adhesion to endothelial cells, extravasation and growth in secondary organs.[3] It can be hypothesized that components of the secondary organ, such as endothelial cells, stromal cells, fibroblasts and parenchymal cells, are functionally organized to promote survival and proliferation of metastasizing cancer cells and generate a favorable microenvironment for cancer cells in metastatic sites.[4,5]

Hypoxia initiates a variety of cellular responses including the activation of hypoxia-inducible factor-1 (HIF-1).[6,7] HIF-1 is a ubiquitously expressed heterodimeric transcription factor composed of a constitutively expressed β subunit and an oxygen-regulated α subunit. Under normal oxygen tension, the α subunit is continuously hydroxylated at conserved prolyl and asparaginyl residues and is targeted for degradation by the von Hippel–Lindau ubiquitin E3 ligase complex.[8] In hypoxia, inhibition of hydroxylation results in the stabilization of HIF-1α and its subsequent nuclear entry, which leads to transcriptional activation of target genes that stimulates angiogenesis, such as vascular endothelial growth factor (VEGF), that controls invasion of cancer cells, such as matrix metalloproteinases (MMPs), and promotes metabolic adaptation to hypoxia.[9] In general, tumor cells grow faster than the rate of angiogenesis so that tumor tissues are characterized by internal hypoxia. Therefore, activation of HIF-1 has been described in a variety of human cancers and their metastases.[10,11] Moreover, although the role of HIF-1α in tumor cell growth has not been fully elucidated, our results and those from other groups have demonstrated that HIF-1α expression in tumor tissues is likely to help tumor cell survival and growth.[12,13]

RNA interference (RNAi) is an evolutionary conserved sequence-specific gene silencing mechanism, which can be triggered by small 21- to 25-nt double-stranded small interfering RNA (siRNA) or short hairpin RNA (shRNA) that is processed in the cell to form siRNA.[14,15] Intravascular injection of a large-volume isotonic solution at a high speed is a very efficient method for delivering any solutes, including siRNA- and shRNA-expressing plasmid DNA (pDNA), to liver cells. This procedure, the so-called hydrodynamics-based procedure, has been applied to suppress expression of target genes in the liver.[16,17] In addition to such application, we found that the hydrodynamic

Correspondence: Professor Y Takakura, Department of Biopharmaceutics and Drug Metabolism, Graduate School of Pharmaceutical Sciences, Kyoto University, Sakyo-ku, Kyoto 606-8501, Japan.
E-mail: takakura@pharm.kyoto-u.ac.jp
Received 2 August 2007; revised 4 December 2007; accepted 5 December 2007

administration is also applicable to deliver siRNA- and shRNA-expressing pDNA to tumor cells in the liver.[18] Therefore, the hydrodynamics-based procedure can be an effective method to suppress the growth of tumor cells that are metastasized to the liver. Because the hydrodynamic administration can induce RNAi in both tumor cells in the liver and normal liver cells, suppressing the increased expression of a gene that aggravates the metastatic tumor growth in both tumor and liver cells can be an effective approach in treating hepatic metastasis. To this end, we selected HIF-1α as such a target gene in the present study. We applied the hydrodynamic injection method to administer shRNA-expressing pDNA targeting HIF-1α (pshHIF-1α) and found that the suppression of HIF-1α expression in the liver can suppress the growth of metastasizing tumor cells in that organ. Moreover, selective suppression of HIF-1α expression only in normal liver cells was found to be also effective in inhibiting metastatic tumor growth, indicating that HIF-1α expression in normal cells assisted the tumor progression.

Results

Reduction in protein expression of HIF-1α by shRNA-expressing pDNA

As previously reported by several groups, an enzyme-linked immunosorbent assay (ELISA) analysis showed that addition of $CoCl_2$ increased the amount of HIF-1α proteins in Colon26 and B16-BL6 cells (Figure 1a). Similar results were obtained when HIF-1α protein levels in Colon26 cells were evaluated by western blot analysis (Figure 1b). Transfection of pshHIF-1α reduced the amount of HIF-1α protein, whereas transfection of control pDNA or pshGFP (green fluorescent protein) hardly affected the level of HIF-1α expression.

Using immunofluorescent staining with HIF-1α-specific antibody, localization of HIF-1α protein in the cells was visualized. While a weak signal of HIF-1α was observed in cytoplasm when cells were incubated without $CoCl_2$, incubation of Colon26 cells with $CoCl_2$ resulted in nuclear accumulation of HIF-1α, which was detected as yellow signals as a result of overlap between the green fluorescence derived from HIF-1α and the red fluorescence derived from nuclear staining (Figure 1c). Transfection of pshHIF-1α reduced the number of cells that show HIF-1α accumulation in their nucleus.

Inhibition of HIF-1 transcriptional activity by pshHIF-1α

To investigate whether pshHIF-1α is effective in suppressing the transcription activity of HIF-1, cells were transfected with a pDNA encoding luciferase gene under the control of hypoxia response element (HRE). In Colon26 cells, HRE-dependent luciferase expression from the reporter pDNA co-transfected with control pDNA or pshGFP was moderately increased by the addition of $CoCl_2$. However, in B16-BL6 cells, HRE-dependent luciferase expression was increased by the addition of $CoCl_2$ compared with Colon26 cells (Figures 2a and b). HRE-dependent luciferase expression in the presence of $CoCl_2$ was almost completely inhibited to about the expression level observed in the absence of $CoCl_2$ by transfection of pshHIF-1α.

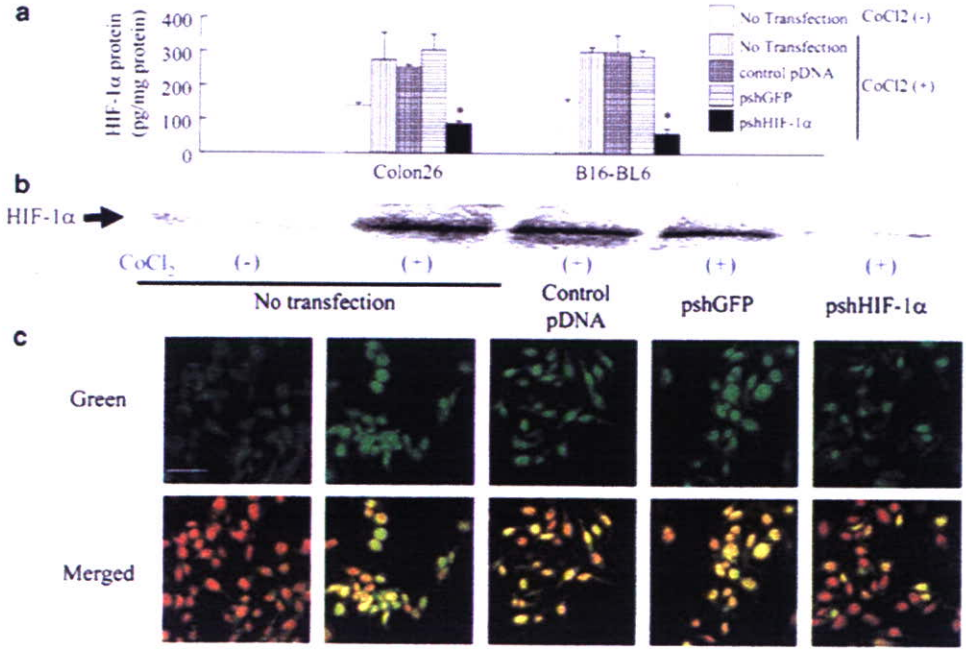

Figure 1 Hypoxia-inducible factor-1α (HIF-1α) protein expression level in tumor cells following transfection of short hairpin (shRNA)-expressing plasmid DNA (pDNA). Cells were transfected with control pDNA, pshGFP (green fluorescent protein) or pDNA expressing shRNA targeting HIF-1α (pshHIF-1α). At 4 h after transfection, cells were washed with phosphate-buffered saline (PBS) and then cultured with growth medium supplemented with or without 100 μM $CoCl_2$ for an additional 20 h. (**a**) Enzyme-linked immunosorbent assay (ELISA) analysis of HIF-1α protein from cell lysates of Colon26 or B16-BL6 cells. The results are expressed as the mean ± s.d. of three samples. $^*P < 0.05$ for Student's *t*-test versus the control group. (**b**) Western blotting analysis of HIF-1α for cell lysates of Colon26 cells. (**c**) Immunofluorescent staining of HIF-1α in transfected Colon26 cells. HIF-1α protein expression was detected as a green color, and the cell nucleus was stained with propidium iodide (red). Yellow signals indicate that HIF-1α localizes in the cell nucleus. Scale bar = 50 μm.

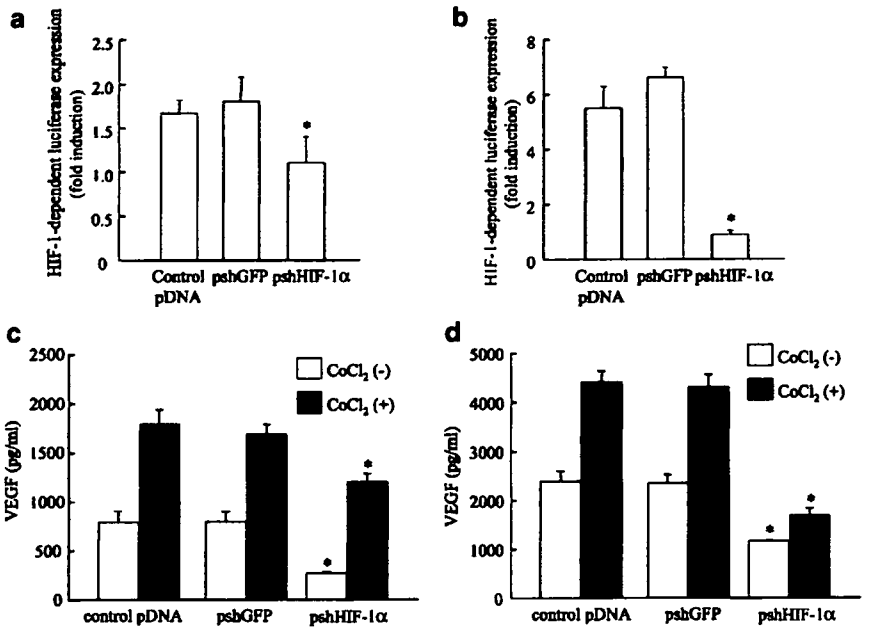

Figure 2 Suppression of hypoxia-inducible factor-1 (HIF-1)-dependent gene expression by transfection of plasmid DNA (pDNA) expressing shRNA targeting HIF-1α (pshHIF-1α). (a, b) Suppression of HIF-1-dependent reporter gene expression by pshHIF-1α. pLuc-HRE and phRL-TK were co-transfected with control pDNA, pshGFP (green fluorescent protein) or pshHIF-1α to Colon26 (a) or B16-BL6 (b) cells. At 4 h after transfection, cells were washed with phosphate-buffered saline (PBS) and cultured in medium with or without 100 μM $CoCl_2$ for an additional 20 h. Luciferase activities were measured 24 h after transfection. The results are expressed as the mean ± s.d. of three samples. (c, d) Reduction in HIF-1-dependent vascular endothelial growth factor (VEGF) production by pshHIF-1α. Colon26 (c) or B16-BL6 (d) cells were transfected with control pDNA, pshGFP or pshHIF-1α. At 4 h after transfection, cells were washed with PBS and cultured in medium with or without 100 μM $CoCl_2$ for an additional 44 h. The amount of VEGF protein in the cultured medium was measured 48 h after transfection using enzyme-linked immunosorbent assay (ELISA). The results are expressed as the mean ± s.d. of three samples. *$P<0.05$ for Student's *t*-test versus the control group.

To further estimate the effect of pshHIF-1α transfection on the expression of VEGF, an endogenous gene product of HIF-1 transcription activity, culture media of tumor cells were collected 48 h after the transfection. The VEGF concentration in the supernatant was measured by ELISA (Figures 2c and d). In both cell lines, about a two-fold increase was detected in the VEGF from $CoCl_2$-treated cells compared with that from untreated cells. In Colon26 cells, transfection of pshHIF-1α reduced VEGF secretion to about one-third or two-thirds of the control values without or with $CoCl_2$, respectively. In B16-BL6 cells, transfection of pshHIF-1α reduced VEGF secretion to about half or one-third of the control values without or with $CoCl_2$, respectively.

Increase in HIF-1α expression in the liver by tumor inoculation via the portal vein

Mice were inoculated with tumor cells into the portal vein, and received an intravenous injection of each pDNA 5 days after tumor inoculation. Then, immunofluorescent staining of liver sections was performed to detect HIF-1α protein expression 7 days after tumor inoculation. Representative images are shown in Figures 3a–g. No significant signal of HIF-1α was observed in the liver sections of naïve mice, sham-operated mice and those receiving control pDNA (Figures 3a–c). In contrast, a strong HIF-1α signal was observed in the liver sections of tumor-bearing mice (Figure 3d). In these pictures, increased HIF-1α expression was mainly observed in hepatic cells. Administration of control pDNA or pshGFP had little effect on HIF-1α expression induced by the inoculation of tumor cells (Figures 3e and f). Moreover, hydrodynamic administration of pshHIF-1α reduced the signal intensity derived from HIF-1α protein compared with other tumor-bearing groups (Figure 3g). By quantitatively analyzing relative areas of the HIF-1α expression (green signal) to the total area in the images, the percentage inhibition by pshHIF-1α was calculated to be about 20–30% of the other tumor-bearing groups. In addition, the administration of pshHIF-1α significantly ($P<0.05$) reduced the mRNA expression of HIF-1α in tumor-bearing liver, from 0.0059 ± 0.0011 copies relative to GAPDH mRNA (the control pDNA-treated group) to 0.0021 ± 0.0005.

Suppression of HIF-1α expression in liver by the pre-administration of pshHIF-1α

As it had been demonstrated that tumor inoculation via the portal vein induced HIF-1α accumulation in liver cells, we investigated whether the delivery of pshHIF-1α only to liver cells, not to tumor cells, affects tumor growth in the liver. To this end, tumor cells were inoculated 3 days after the hydrodynamic administration of pDNAs. Immunofluorescent staining for HIF-1α was performed at 2 days after tumor inoculation to investigate the HIF-1α expression level at that time (Figures 3h–l). Similar to the results of the sample prepared at 7 days after tumor inoculation, a strong signal derived from HIF-1α protein was detected in the liver sections prepared at 2 days after tumor inoculation (Figure 3i).

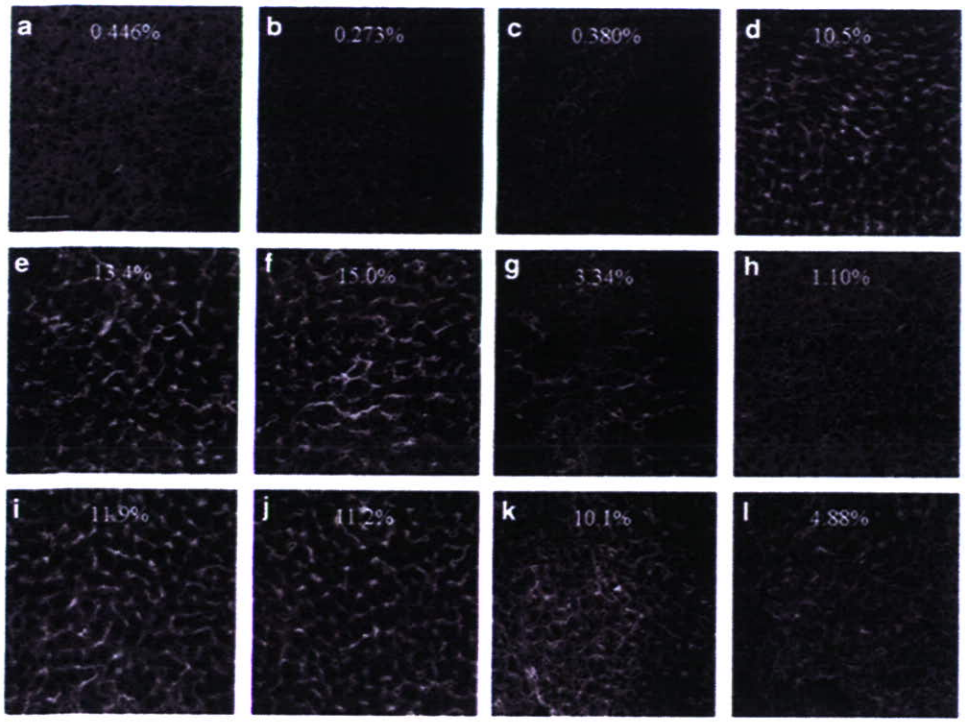

Figure 3 Hypoxia-inducible factor-1α (HIF-1α) expression in the liver of tumor-bearing mice. Some mice were untreated (**a**) or received plasmid DNA (pDNA) only (**b**). The sham operation group (**c**) received only an intraportal injection of Hank's balanced salt solution (HBSS) solution without tumor cells. At 5 days after tumor inoculation via the portal vein, mice were untreated (**d**) or received an intravenous injection of control pDNA (**e**), pshGFP (green fluorescent protein) (**f**) or pDNA expressing shRNA targeting HIF-1α (pshHIF-1α) (**g**). At 2 days after pDNA administration, liver samples were collected and subjected to immunostaining for HIF-1α. The sham operation group received only an intraportal injection of HBSS solution without tumor cells (**h**). At 3 days before tumor inoculation via the portal vein, mice were untreated (**i**) or received an intravenous injection of control pDNA (**j**), pshGFP (**k**) or pshHIF-1α (**l**). At 2 days after tumor inoculation, liver samples were collected and subjected to immunostaining for HIF-1α. Scale bar = 50 μm. Numbers in the images represent the relative area of HIF-1α expression (green signal) to the total area. See online version for color figure.

pshHIF-1α administrated before tumor inoculation suppressed the induction of HIF-1α expression by tumor inoculation (Figure 3l). Administration of irrelevant pDNAs did not change the expression level of HIF-1α in the liver (Figures 3j and k). Quantification of the relative areas of the HIF-1α expression (green signal) to the total area in the images indicated that pre-administration of pshHIF-1α reduced HIF-1α expression to about 50% of the other tumor-inoculated groups.

Location of HIF-1α expression in the tumor-inoculated liver relative to tumor cells

To visualize Colon26 cells in the liver, Colon26 cells transfected with pDsRed2-N1 were inoculated into the portal vein of mice. Immunofluorescent staining for HIF-1α was performed at 2 days after tumor inoculation to investigate the location of HIF-1α expression relative to tumor cells (Figures 4a–d). DsRed-labeled Colon26 cells were found in some liver sections, and almost all of these cells were surrounded by liver cells expressing an increased level of HIF-1α (Figures 4a and b). Some liver cells not close to Colon26 cells also showed a high HIF-1α expression (Figure 4c), but most other liver cells hardly expressed the protein (Figure 4d). These results suggest that tumor cells entrapped in the hepatic capillaries is closely associated with the increased expression of HIF-1α in the surrounding liver cells.

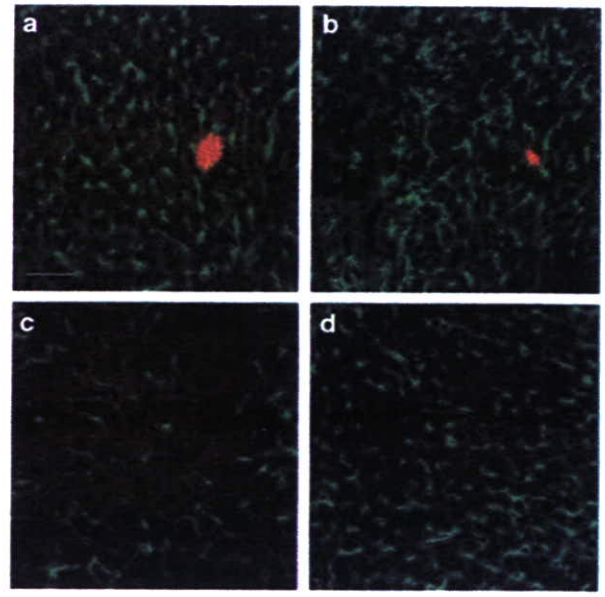

Figure 4 Location of hypoxia-inducible factor-1α (HIF-1α) expression in the tumor-bearing liver relative to tumor cells. At 2 days after tumor inoculation, liver samples were collected and subjected to immunostaining for HIF-1α. Red signals represent Colon26 cells expressing DsRed, and green signals represent HIF-1α protein. Representative images of liver sections positive (**a**, **b**) or negative (**c**, **d**) for DsRed-labeled Colon26 cells are indicated. Scale bar = 50 μm.

Induction of MMP-2 and -9 expression in the liver by tumor inoculation via the portal vein

To evaluate the effect of tumor inoculation via the portal vein on the MMP expression in the liver, the amount of MMP in liver homogenate was measured by gelatin zymography 8 days after tumor inoculation (Figure 5a). As we have reported previously, MMP-2 and -9 activities in the homogenate of tumor-inoculated liver was higher than that of the untreated group. A hydrodynamic delivery of control pDNA or pshGFP 5 days after tumor inoculation had little or no effect on both types of MMP activity. No significant increase in the MMP activity was detected in the liver homogenate of sham-operated mice or mice that received only pDNA. Intravenous injection of pshHIF-1α by the hydrodynamics-based procedure 5 days after tumor inoculation clearly reduced the MMP-9 gelatinolytic activity in the liver of tumor-bearing mice compared with the other tumor-inoculated group. Less, but detectable, reduction was also observed in the MMP-2 activity.

To assess the effect of HIF-1α expression in normal cells on MMP production, pshHIF-1α was administered 3 days before tumor inoculation. Gelatin zymography was performed at 3 days after tumor inoculation (Figure 5b). At this time point, the sham operation group showed slightly increased MMP-9 activity compared with naïve mice. Although the increase in MMP-9 expression level in the liver at this time was smaller than that detected at 8 days after tumor inoculation, the homogenate of tumor-bearing liver showed a higher MMP-9 activity than the other tumor-free groups. Pretreatment of pshHIF-1α reduced MMP-9 induction by tumor inoculation, while preinjection of control pDNA and

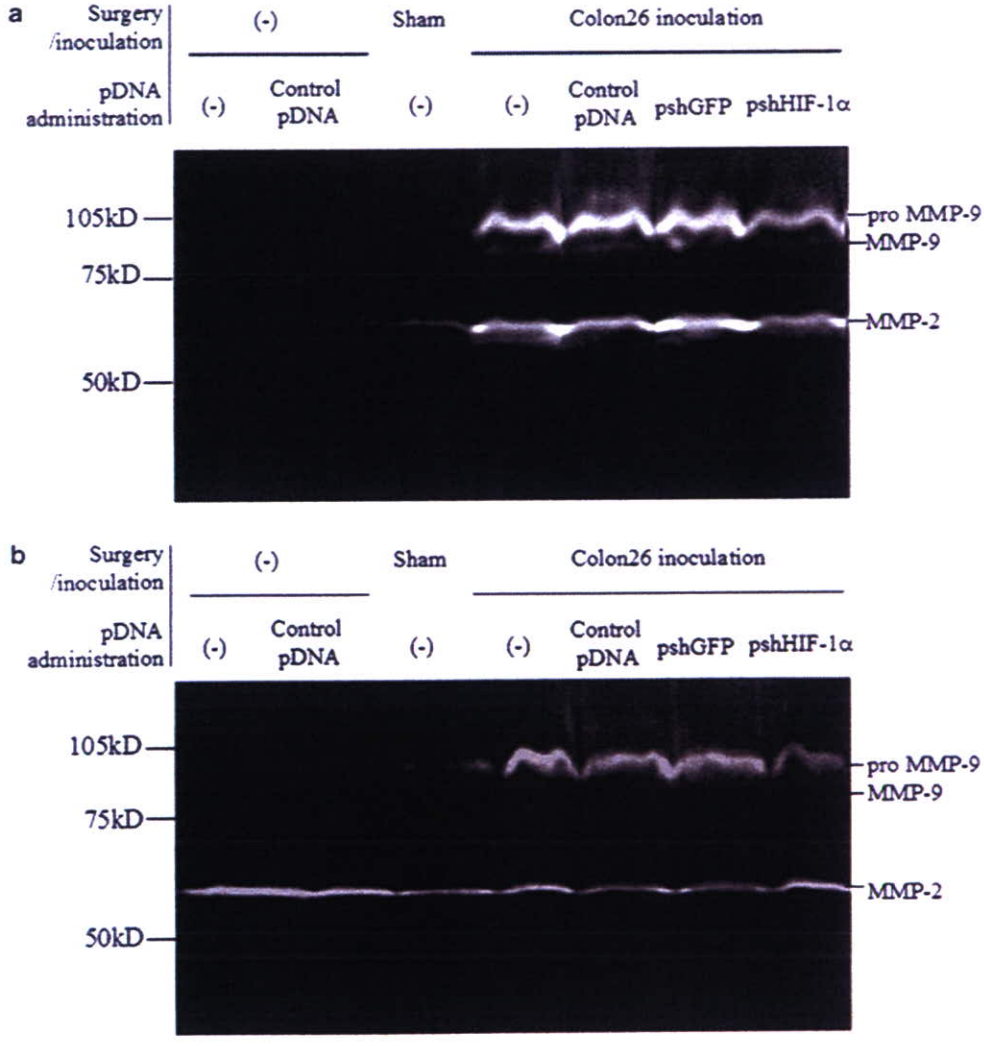

Figure 5 Gelatin zymography performed on liver samples. (**a**) At 5 days after tumor inoculation via the portal vein, mice received an intravenous injection of control plasmid DNA (pDNA), pshGFP (green fluorescent protein) or pDNA expressing shRNA targeting HIF-1α (pshHIF-1α). The sham operation group received only an intraportal injection of Hank's balanced salt solution (HBSS) solution without tumor cells. At 3 days after pDNA administration, liver samples were collected and subjected to gelatin gel zymography. Four mice of each group were used to analyze the matrix metalloproteinase (MMP) expression, and typical results are shown. (**b**) At 3 days before tumor inoculation via the portal vein, mice received an intravenous injection of control pDNA, pshGFP or pshHIF-1α. The sham operation group received only an intraportal injection of HBSS solution without tumor cells. At 3 days after tumor inoculation, liver samples were collected and subjected to gelatin gel zymography. Four mice of each group were used to analyze the MMP expression, and typical results are shown.

pshGFP had little effect on MMP-9 induction in the liver following tumor inoculation. We did not observe any obvious difference in MMP-2 production between tumor-free and tumor-bearing groups.

Suppression of metastatic tumor growth in the liver by pshHIF-1α

Figure 6a shows the tumor cell number in the liver, which was evaluated by measuring tumor-derived luciferase activities at 1 week after pDNA administration (Figure 6a). Mice were inoculated with Colon26 cells into the portal vein, and each pDNA was injected into the tail vein with 5-day interval. Control pDNA or pshGFP hardly reduced the number of tumor cells, while pshHIF-1α significantly ($P<0.05$) reduced the number to about, on average, 1–2% of the other groups. Many large tumor nodules were found in the frozen liver sections of mice receiving control pDNA (Figure 6c). In a quite contrast, much small and few tumor nodules were detected in the sections of mice receiving pshHIF-1α (Figure 6d). These hematoxylin and eosin-stained sections strongly support the quantitative results of metastatic tumor growth estimated using the luciferase activity of Colon26/Luc cells (Figure 6a).

Next, we investigated the effect of preadministration of pshHIF-1α on the growth of tumor cells in the liver by estimating the tumor cell number 12 days after tumor inoculation (Figure 6b). As a result, pshHIF-1α preadministration 3 days before tumor inoculation significantly reduced the number of tumor cells in the liver 12 days after tumor inoculation compared with the groups that were untreated or given pDNA. On average,

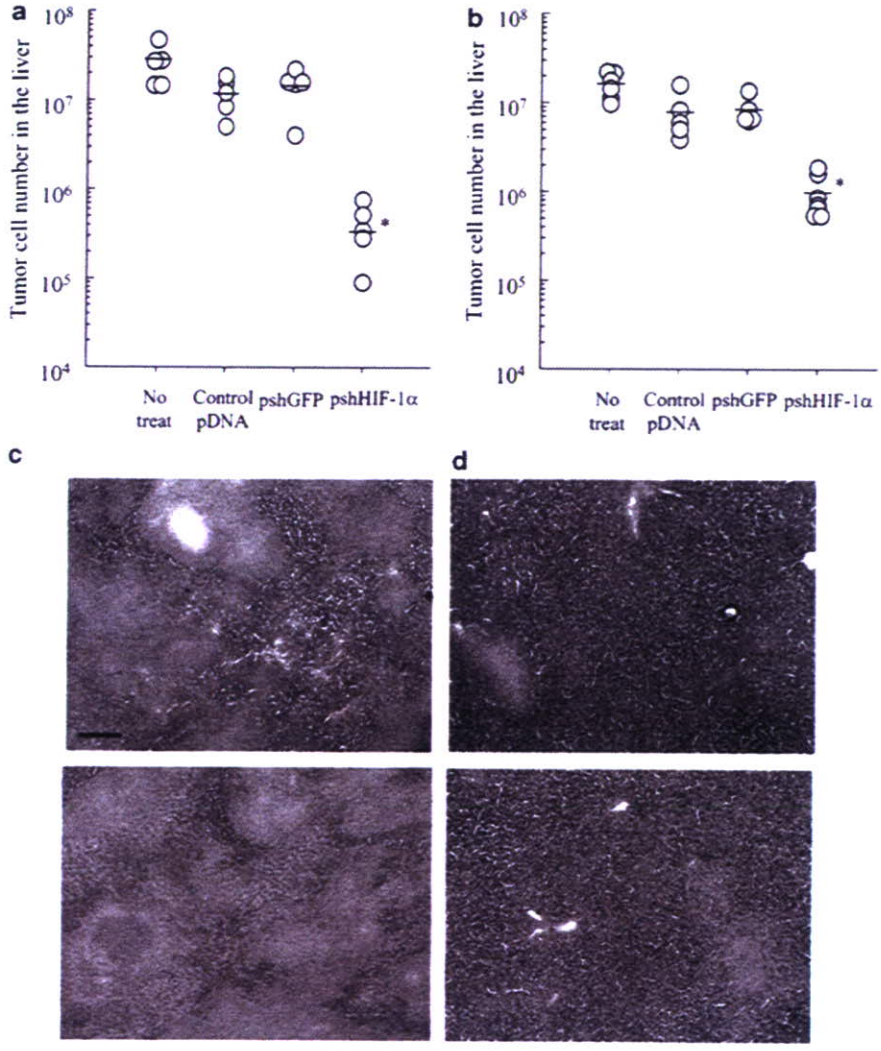

Figure 6 Number of Colon26/Luc cells in mouse liver 12 days after tumor inoculation. (**a**) At 5 days after tumor inoculation via the portal vein, mice received an intravenous injection of control plasmid DNA (pDNA), pshGFP (green fluorescent protein) or pDNA expressing shRNA targeting HIF-1α (pshHIF-1α). At 7 days after pDNA administration, liver samples were collected and the number of tumor cells was evaluated by measuring luciferase activities derived from Colon26/Luc cells. Open circles (○) indicate the tumor cell number in the liver of individual mice. Bars indicate the average tumor cell number of each group ($n=5$). *$P<0.05$ for Student's *t*-test versus untreated group. (**b**) At 3 days before tumor inoculation via the portal vein, mice received an intravenous injection of control pDNA, pshGFP or pshHIF-1α. At 12 days after tumor inoculation, liver samples were collected and the number of tumor cells was evaluated by measuring luciferase activities derived from Colon26/Luc cells. Open circles (○) indicate the tumor cell number in the liver of individual mice. Bars indicate the average tumor cell number of each group of at least five mice. *$P<0.05$ for Student's *t*-test versus untreated group. (**c**, **d**) Hematoxylin and eosin-stained liver sections of tumor-bearing mice receiving (**c**) control pDNA or (**d**) pshHIF-1α at 7 days after tumor inoculation. Scale bar = 200 μm. See online version for color figure.

preadministration of pshHIF-1α reduced the number of tumor cells to about 10% of other groups. The degree of reduction in the number of tumor cells by pshHIF-1α administered before tumor inoculation was about 5- to 10-fold less than that of pshHIF-1α administered after tumor inoculation.

Discussion

HIF-1α expression and subsequent HIF-1 activation in cancer cells play important roles in cancer progression by controlling the gene expression related to cancer cell proliferation, apoptosis and metastasis.[9] In the present study, we demonstrated that HIF-1α expression in normal hepatic cells is also increased by tumor cells entering the liver via the portal vein and that such HIF-1α expression aggravates tumor growth. Our results indicate the possibility of a novel therapeutic strategy for inhibiting metastatic tumor growth by silencing the HIF-1α expression in both normal and tumor cells.

Suppression of nuclear accumulation of HIF-1α by pshHIF-1α (Figure 1) was followed by inhibition of HIF-1-dependent transcription activities (Figure 2). In the experiment using pLuc-HRE, pshHIF-1α suppressed the transcription activity to almost the basal level in both Colon26 and B16-BL6 cells. Such an efficient inhibitory effect on luciferase expression might be because pLuc-HRE was co-transfected with pshHIF-1α, by which both pDNAs were delivered to the same cells. On the other hand, the suppressive effect of pshHIF-1α on VEGF production from B16-BL6 cells was much greater than that from Colon26 cells. Two factors may explain the difference in the efficiency of the inhibitory effect on VEGF production between B16-BL6 cells and Colon26 cells. One is the transfection efficiency of the pshHIF-1α. By using pDNA expressing enhanced green fluorescent protein (EGFP), we found that the transfection efficiency to B16-BL6 and Colon26 cells was about 80–90 and 70–80%, respectively, at 24 h after transfection (Y Takahashi *et al.*, unpublished data). Therefore, the difference in transfection efficiency between B16-BL6 and Colon26 cells may be one reason for the difference in suppressive effect on VEGF production by pshHIF-1α. The other reason for the difference in suppression in the two cell lines could be the contribution of HIF-1-dependent VEGF production to the total VEGF production. Other hypoxia-inducible transcriptional factors, such as HIF-2, are also known to be activated by $CoCl_2$ and increased HIF-2 expression might result in VEGF expression.[19]

When tumor cells were inoculated via portal vein, HIF-1α protein expression was increased in tumor-bearing liver (Figure 3). Inoculation of DsRed-labeled Colon26 cells clearly demonstrated that liver cells close to the tumor cells expressed HIF-1α at a high level (Figure 4). Oxygen concentration-dependent and -independent pathways might be considered as the mechanism for such an increase in HIF-1α expression. When tumor cells are inoculated via the portal vein, tumor cells are first arrested in small vessels, followed by extravasation, invasion of tissues and proliferation of tumor cells.[3] Therefore, blood flows would be, at least transiently, hindered by tumor cells, which could result in a reduction in the oxygen supply. In addition to hypoxia, other processes such as growth factor stimulation and cytokine stimulation are reported to increase HIF-1α expression and activate HIF-1-dependent transcription.[9,20] When tumor cells metastasize to the liver, expression of these secretary proteins might be induced and result in increased HIF-1α expression.

To distinguish the role of HIF-1α expressed in tumor cells from that in normal liver cells, pshHIF-1α was administered 3 days before tumor inoculation. As pDNA injected into the systemic circulation is very quickly degraded by nucleases and cleared by Kupffer and sinusoidal endothelial cells,[21] pDNA injected would have hardly any effects on the expression level of HIF-1α in Colon26/Luc cells. On the other hand, when pshHIF-1α was administered after tumor inoculation, pshHIF-1α might be delivered to both tumor and liver cells.[18] Therefore, pshHIF-1α administered before tumor inoculation might have been delivered only to normal cells in the liver, while pshHIF-1α administered after tumor inoculation might have been delivered to both tumor and normal cells in the liver.

In a previous study, we reported that Colon26 cell inoculation via the portal vein increased MMP-9 expression in the liver.[22] Elezkurtaj *et al.*[23] demonstrated that intrasplenic inoculation of CT-26 colon carcinoma cells, which form experimental liver metastases, increased MMP-2 and -9 expressions in liver tissue. In agreement with these results, we have found that MMP-9 is generated mainly from host cells, not the inoculated tumor cells (Y Takahashi *et al.*, unpublished data). There are some published papers reporting that MMP-9 expression is directly or indirectly regulated by HIF-1.[24–26] Therefore, we hypothesized that increased HIF-1 transcription activity in normal cells in the liver contributes to MMP-9 production induced by tumor cell inoculation. Intravenous administration of pshHIF-1α was effective in reducing the expression of MMP-9 after tumor inoculation, which indicates that HIF-1 expression in tumor cells and normal cells in the liver might play an important role in MMP-9 production. Moreover, administration of pshHIF-1α before tumor inoculation was found to be also effective in reducing the amount of MMP-9 in the liver. This result reinforces the hypothesis that normal cells in the liver, not tumor cells, are the major producer of MMP-9 and that MMP-9 expression is regulated by HIF-1. Although its role in metastatic tumor cell growth is still unclear, increased MMP expression is frequently accompanied by tumor metastasis and suppression of MMP expression could be used as a growth inhibitory treatment to prevent tumor metastasis.[23,27,28]

When pshHIF-1α was administered to tumor-bearing mice by the hydrodynamics-based procedure, a significant reduction in the number of tumor cells was observed (Figure 6a). This result indicates that HIF-1α expression in either tumor cells or hepatic normal cells or in both types of cells plays an important role in tumor progression. A histological study of the liver sections confirmed that the administration of pshHIF-1α significantly reduced the metastatic tumor growth in the liver (Figures 6c and d). Preadministration of pshHIF-1α reduced the tumor cell number in the liver at 12 days after tumor inoculation compared with the other groups (Figure 6b). This result implies that HIF-1α expression in the normal cells in the liver might play an important role in tumor cell growth in the liver, although the reduction